Passive Imaging and monitoring: disorder and correlation.

Michel Campillo
ISTerre (Grenoble)

European Research Council
erc
Whisper
Towards continuous monitoring of the continuously changing Earth

ISTerre
Institut des Sciences de la Terre

UNIVERSITÉ Grenoble Alpes

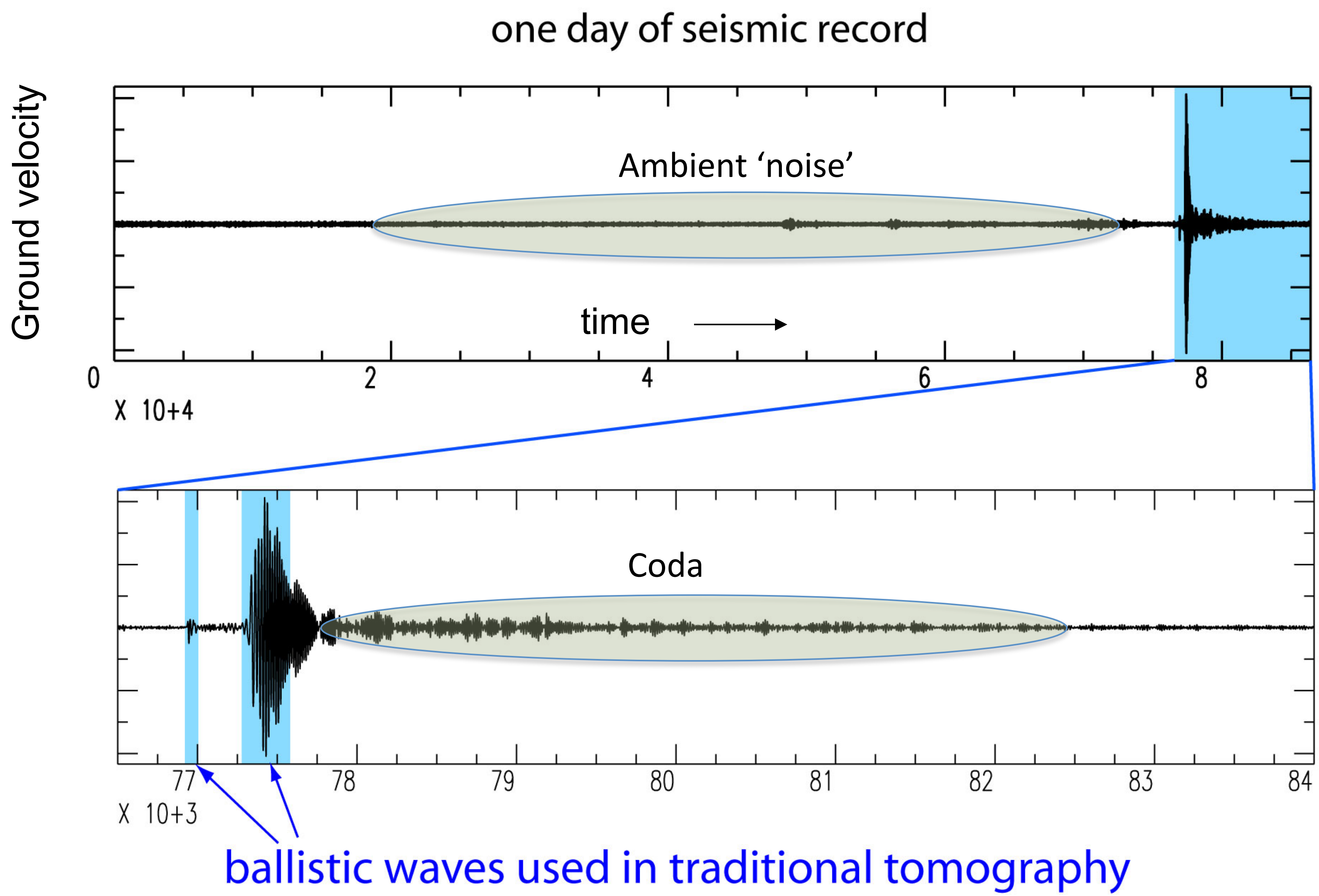

one day of seismic record
Ground velocity
Ambient 'noise'
time
0
2
4
6
8
X 10+4
Coda
77
78
79
80
81
82
83
84
X 10+3
ballistic waves used in traditional tomography

The origin of the noise in the period band 5-10s as seen by seismic arrays

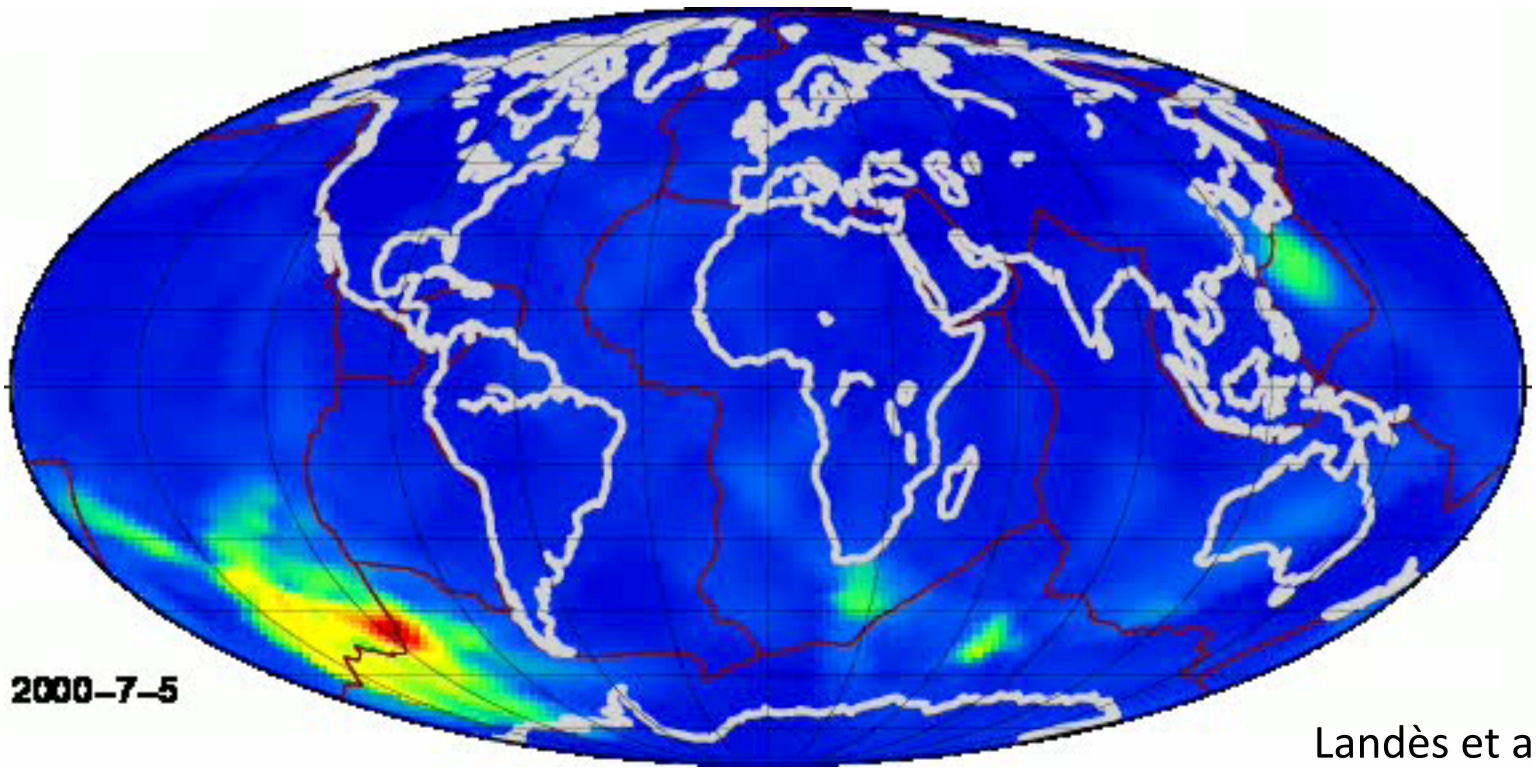

Landès et al., 2010

VARIABLE SOURCE LOCATIONS

At higher frequencies: human activity, wind,….

Global ‘noise’ sources in the microseism band
(extended ≈2-50s)

Strong contribution from oceanic waves

Example of a global comparison
(secondary microseism-
Miche/Longuet-Higgins mechanism)

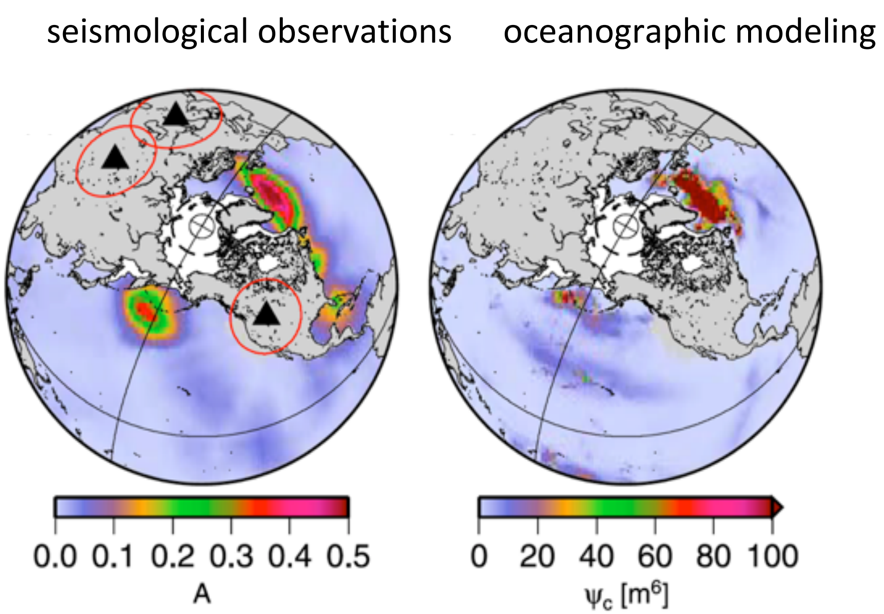

Hillers et al., 2012

Longer periods: infragravity waves, e.g Fukao et al. 2010

+EARTHQUAKES

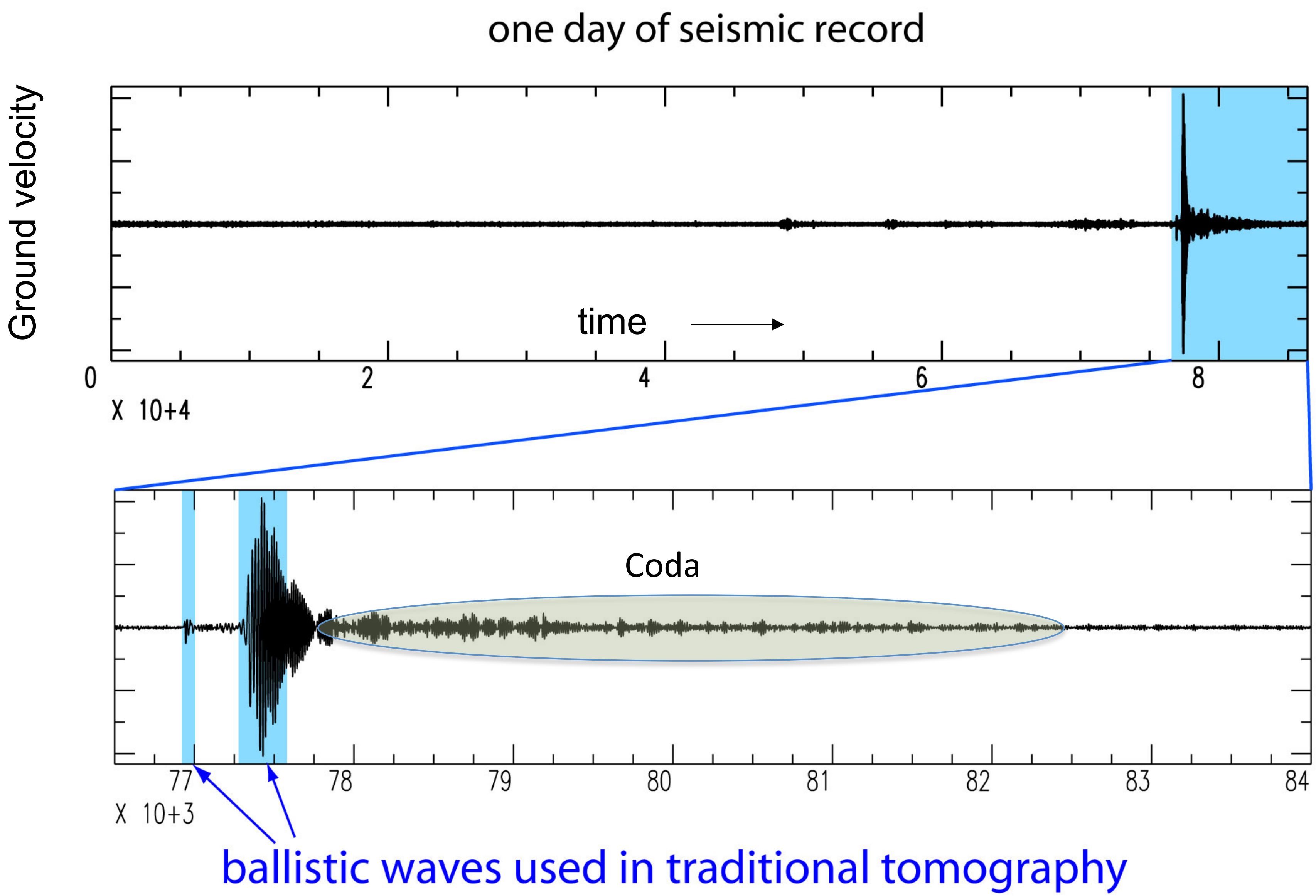

one day of seismic record
Ground velocity
time
0
2
4
6
8
X 10+4
Coda
77
78
79
80
81
82
83
84
X 10+3
ballistic waves used in traditional tomography

A typical record of a local earthquake (0.1-10Hz)

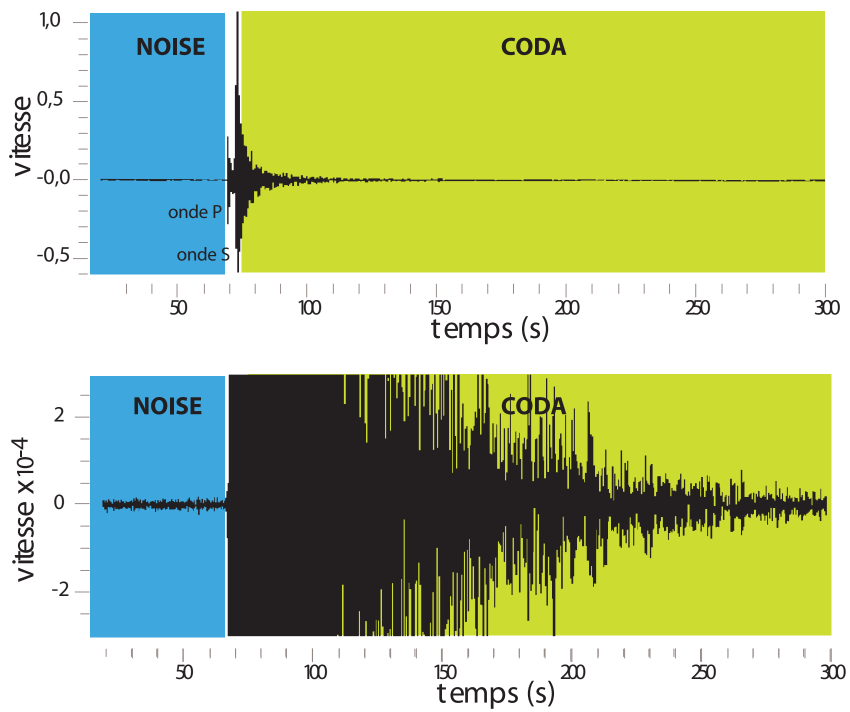

Coda waves = multiply scattered waves (deterministic speckle)

Propagation regimes and description of **energy**

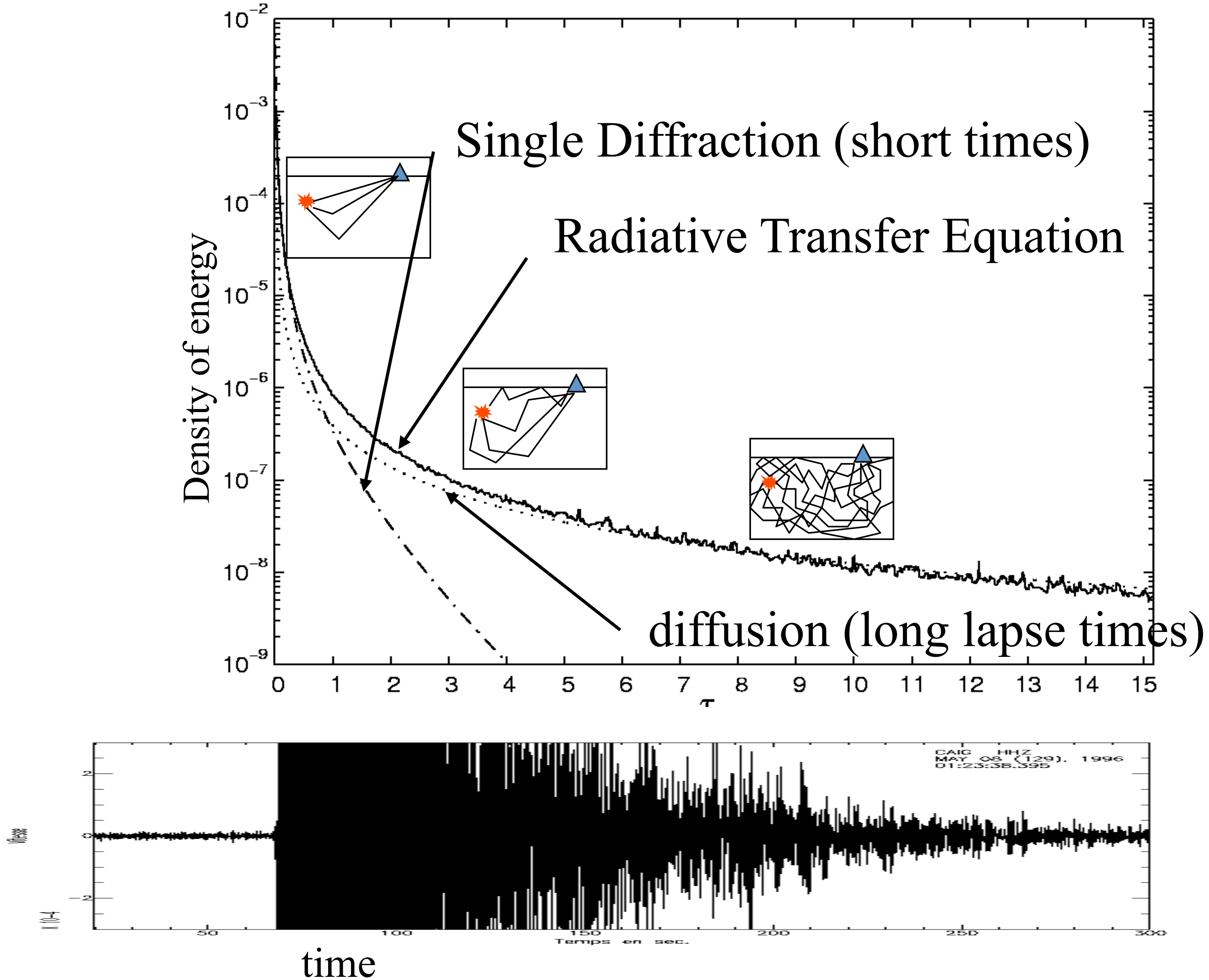

Long continuous records, with components belonging to various propagation regimes (ballistic to diffuse)

Measurements of the wavefield in space and time

➔ Long range field correlations:

Two point time correlation:

$$Corr_{SR}(\tau) = S(t) \otimes R(t) = \int_{-\infty}^{+\infty} S(t)R(t-\tau)dt$$

$$In\,the\,Fourier\,domain : C_{SR}(\omega) = S(\omega).R^{*}(\omega)$$

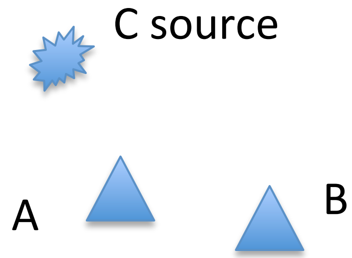

Focusing/virtual source in A

- C source (uncertainties about physics, location..)
- A et B receivers

- Correlation :

$$Corr_{AB}(\tau) = S_{AC}(t) \otimes S_{BC}(t)$$

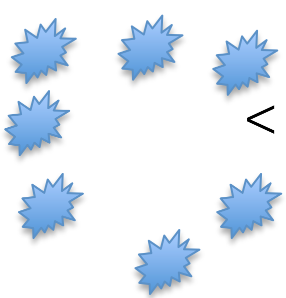

$$< S_{AC}(t) \otimes S_{BC}(t) >_{SOURCES}$$

Derode et al., 2003

Time reversal, correlation and convolution

Convolution

$$Conv_{SR}(t) = S(t) * R(t) = \int_{-\infty}^{+\infty} S(\tau)R(t-\tau)d\tau$$

$$In\,the\,Fourier\,domain : Conv_{SR}(\omega) = S(\omega).\,R(\omega)$$

Time reversal (symmetry of the wave equation)

$$\widehat{R}(t) = R(-t)$$

$$\widehat{R}(\omega) = FT\left[R(-t)\right] = R^{*}(\omega)$$

Correlation and convolution

$$Corr_{SR}(\omega) = S(\omega).R^{*}(\omega) = S(\omega).\widehat{R}(\omega) = Conv_{S\widehat{R}}(\omega)$$

The correlation between two signals is **equal** to the convolution of one signal with the time reversed of the other.

Correlation and Time reversal
Focusing/virtual source in A

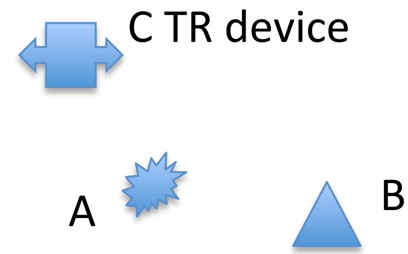

- A source
- C receiver ($S_{AC} = S_{CA}$)
- C emits the time reversed signal
- B receiver
- Convolution :

$$S_{CA}(t) * S_{BC}(-t)$$

$$< S_{CA}(t) * S_{BC}(-t) >_{TIME\ REVERSAL\ DEVICES}$$

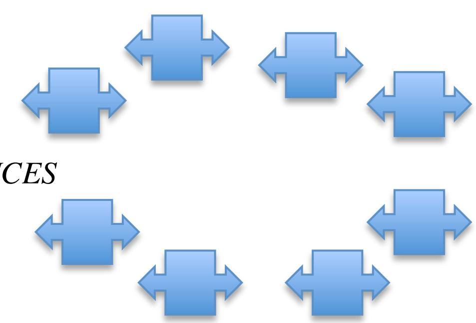

La piscine à Retournement Temporel

From Nicolas Perrez, Petrobras, USPI.

A numerical experiment with an open medium (absorbing boundaries):

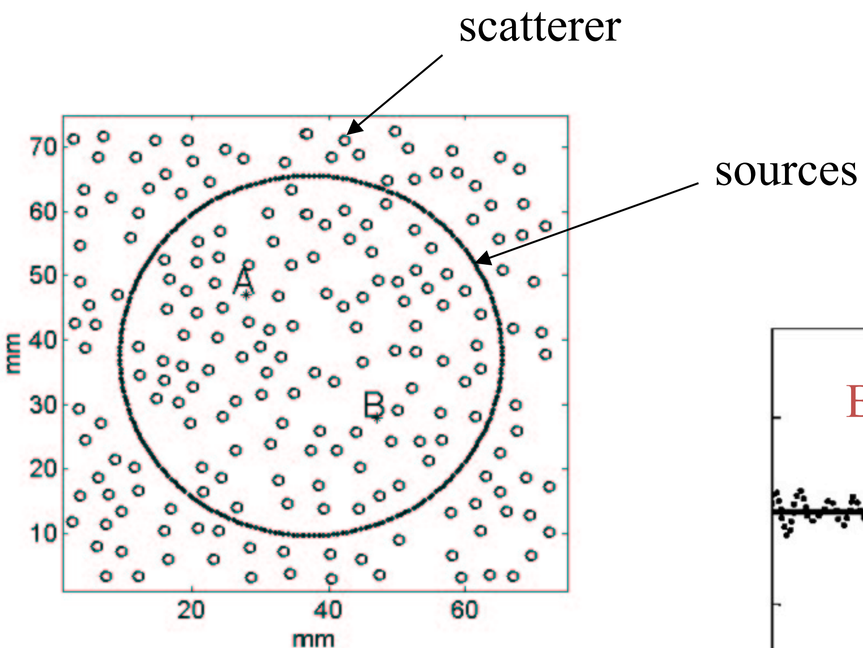

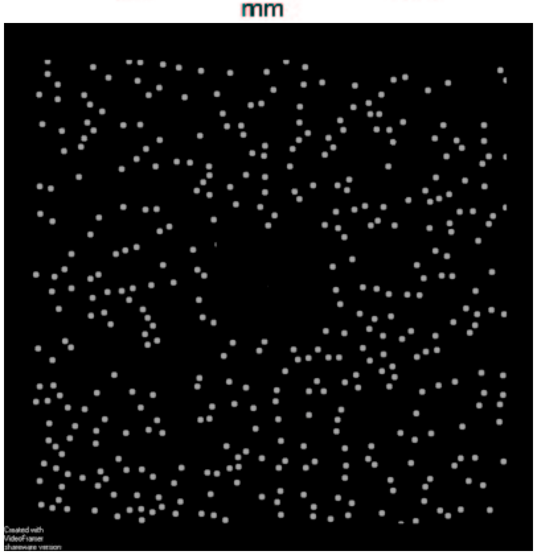

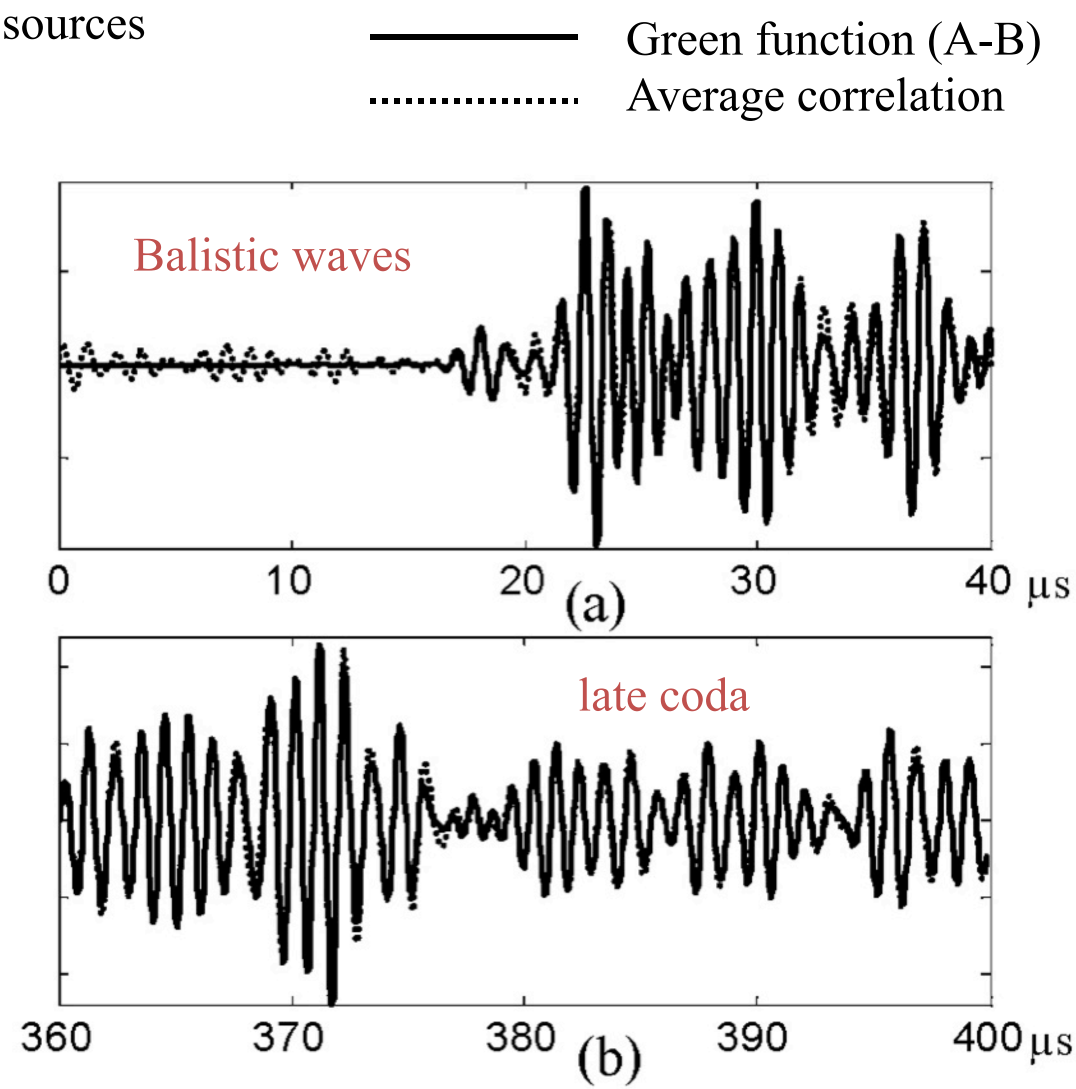

Derode A., E. Larose, M. Campillo and M. Fink (2003)

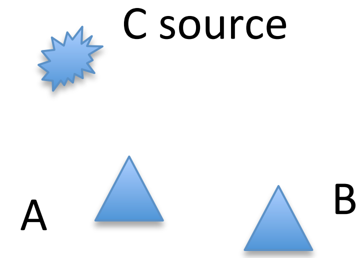

Correlation and Time reversal
Focusing/virtual source in A

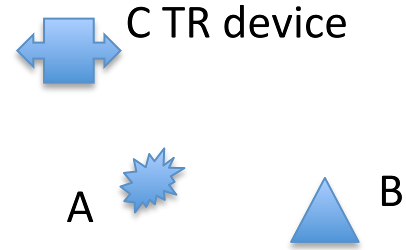

- C source
- A et B receivers

- Correlation

- A source
- C receiver ($S_{AC} = S_{CA}$)
- C emits the time reversed signal
- B receiver
- Convolution :

$$Corr_{AB}(\tau) = S_{AC}(t) \otimes S_{BC}(t) \quad = \quad S_{CA}(t) * S_{BC}(-t)$$

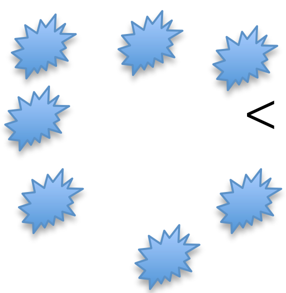

$$< S_{AC}(t) \otimes S_{BC}(t) >_{SOURCES} \quad = \quad < S_{CA}(t) * S_{BC}(-t) >_{TIME\ REVERSAL\ DEVICES}$$

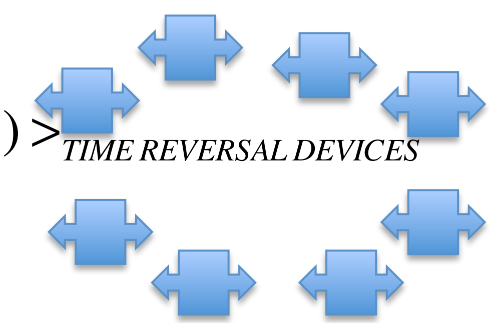

Derode et al., 2003

Ambient noise based method is equivalent to using a (broken) time reversal mirror defined by the sources of ambient noise and the scatterers.

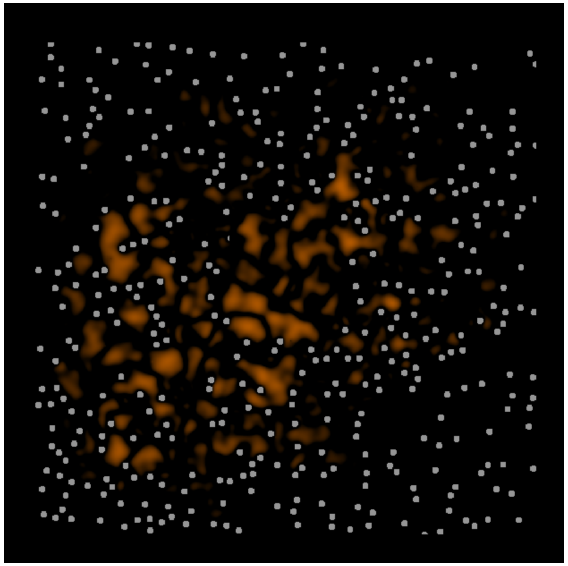

Re-emission from the points 'C' of the time-reversed signals
(map of cross-correlations)

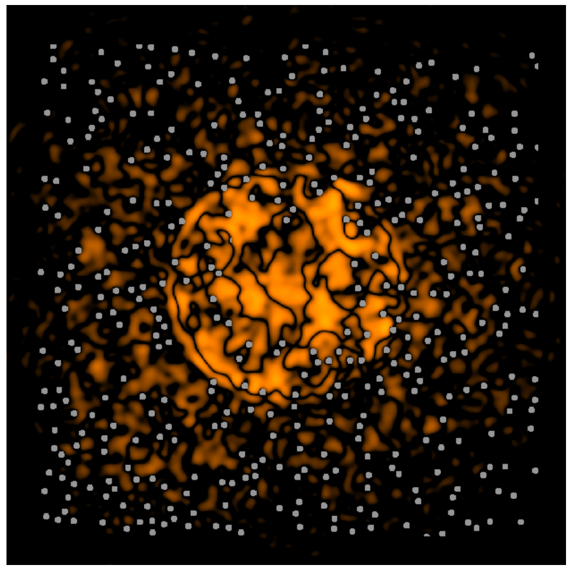

Constructive interferences of time-reversed field

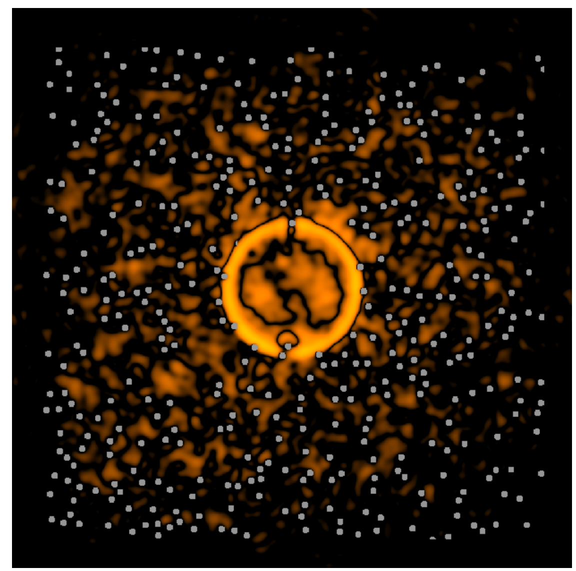

Converging field
: G(-t)

Paul et al, 2005

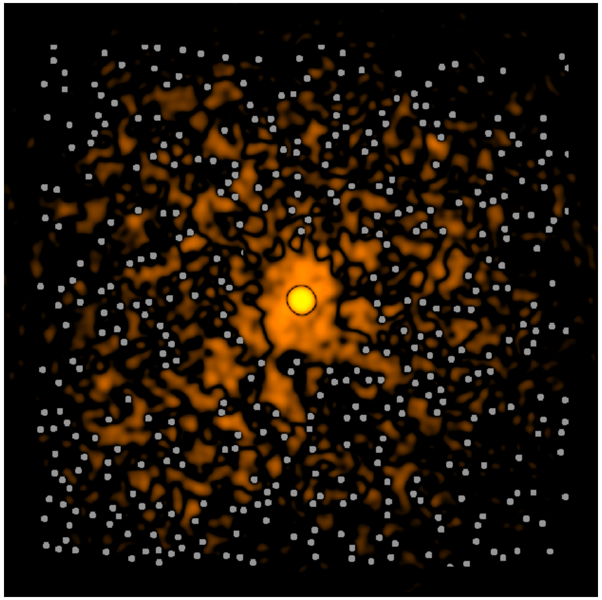

Nearly perfect refocalisation

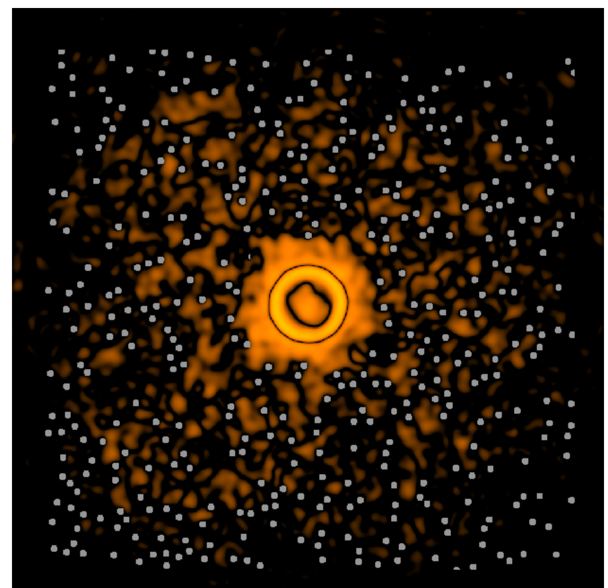

Re-emission from A :
G (t)

Paul et al, 2005

Perspective with a previous appoach.
Spatial autocorrelation coefficient (SPAC):
Average spatial coefficient (2D circular array)

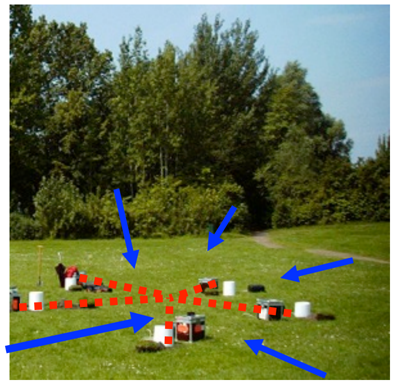

Aki (1957): azimuthal averaged spatial autocorrelation coefficients.
Single mode, plane waves

$$\bar{\rho}(\mathbf{r},\omega_0) = \frac{1}{\pi}\int_0^{\pi} \rho(\mathbf{r},\varphi,\omega_0)\,\mathbf{d}(\theta-\varphi)$$

$$\bar{\rho}(r,\omega_0) = J_0\left(\frac{\omega_0 r}{c(\omega_0)}\right)$$

Azimuthal average could be considered with positions of sensors (the original technique) or under the hypothesis that waves are incident from all directions.

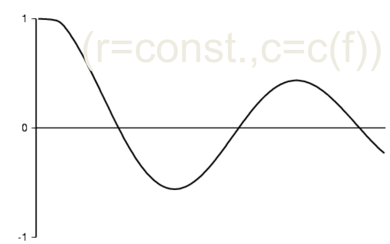

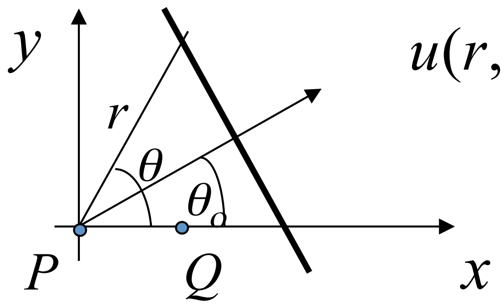

A plane wave in 2D in spectral domain:

$$u(r,\theta,\omega) = F(\omega)\exp(-ikr\cos(\theta-\theta_0))$$

Two point correlation: $$\frac{u^P u^{Q^*}}{|u^P||u^Q|} = e^{+ikr\cos\theta_0}$$

$$\boxed{\langle \rho(r,\omega)\rangle = \left\langle \frac{u^P u^{Q^*}}{|u^P||u^Q|} \right\rangle = \left\langle e^{ikr\cos\theta_0} \right\rangle = \frac{1}{2\pi}\int_0^{2\pi} e^{ikr\cos\theta_0}\, d\theta_0 = J_0(kr)}$$

azimuthal average of the cross-correlation

To be compared with the form of the 2D scalar Green function:

$$G = \frac{1}{4\mathrm{i}\mu} H_0^{(2)}\left(\frac{\omega r}{\beta}\right) = \frac{1}{4\mu}\left\{-Y_0\left(\frac{\omega r}{\beta}\right) - \mathrm{i}J_0\left(\frac{\omega r}{\beta}\right)\right\}$$

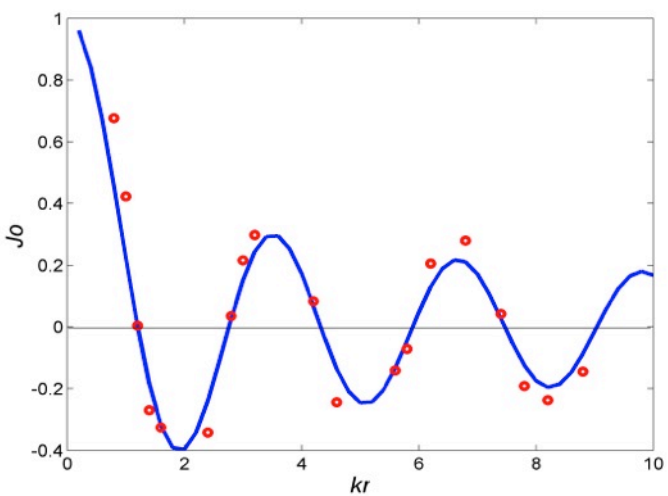

$$\boxed{\mathrm{Im}\left(G_{PQ}\right) = \frac{-1}{4\mu}\left\langle \frac{u_2(P)u_2^*(Q)}{|u_2(P)||u_2(Q)|} \right\rangle}$$

Causality

$$G = \frac{1}{4i\mu} H_0^{(2)}\left(\frac{\omega r}{\beta}\right)$$

$$G = \frac{1}{2\pi\mu} \frac{H\left(t - r/\beta\right)}{\sqrt{t^2 - r^2/\beta^2}}$$

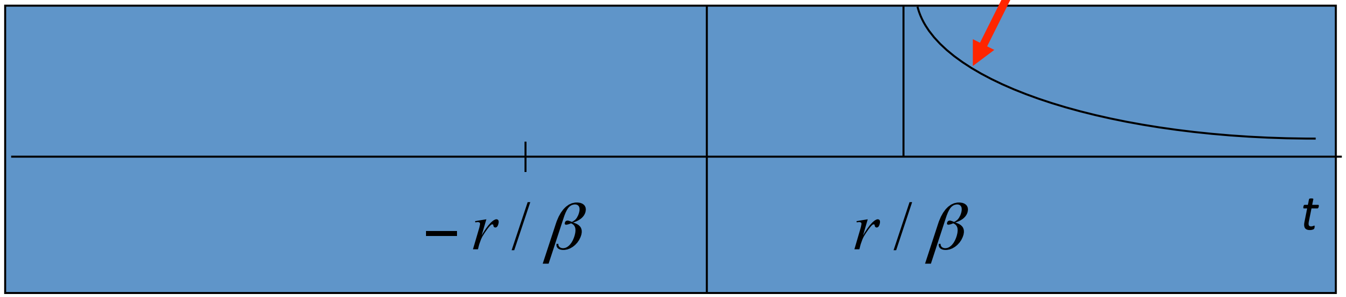

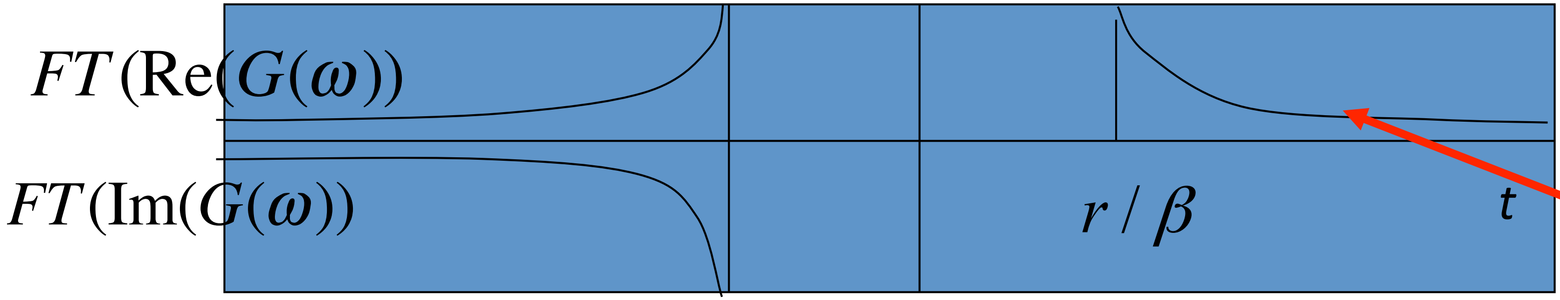

(Im, Re)

G/2

2D single mode (SH,..):

Correlation with isotropic illumination = Green function (+t/-t)

Propagation regimes and description of **energy**

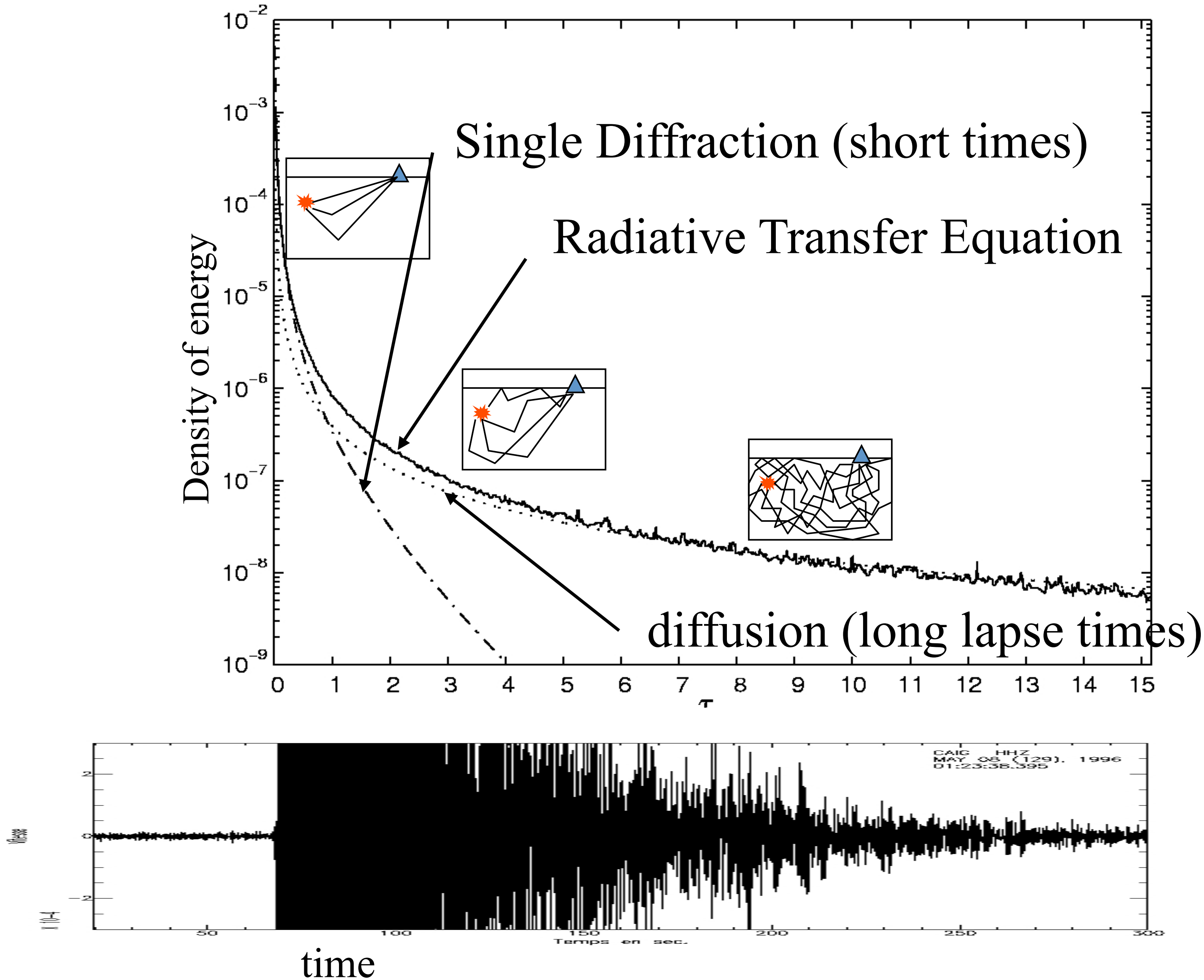

For asymptotically long lapse time (diffusion), the disorder produces a completely randomized wave-field. such that , all the modes of propagation are excited in average to equal energy (the equipartition principle).

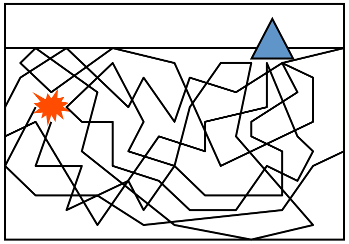

Numerical example:2D scalar waves

➔intensity isotropy

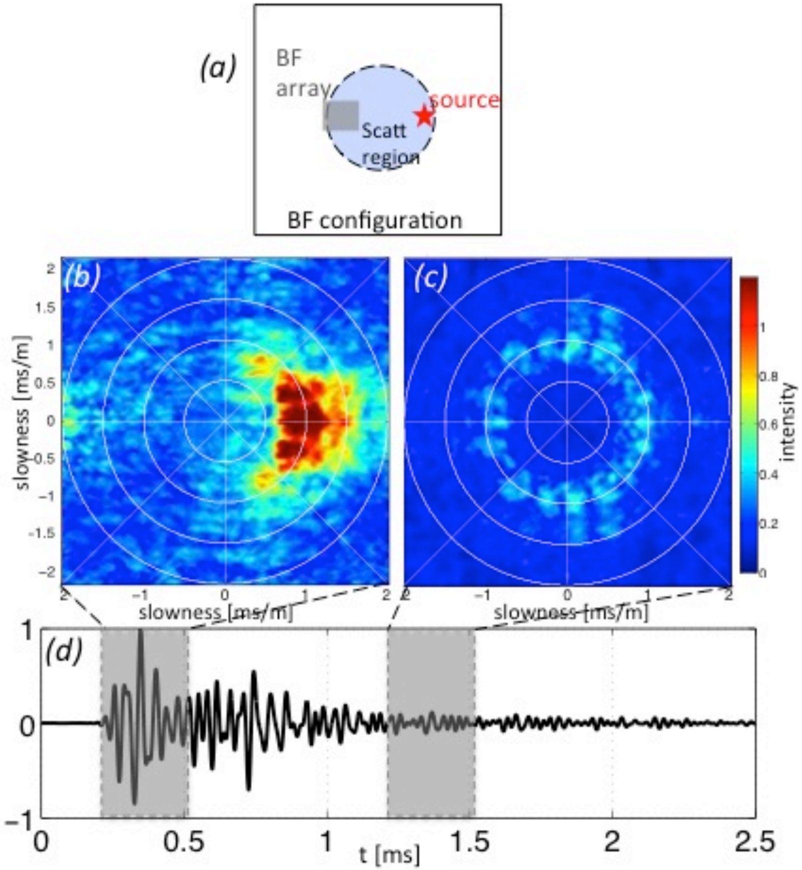

Implication for elastic waves (Weaver, 1982, Ryzhik et al., 1996): P to S energy ratio stabilizes at a value independant of the details of source and scattering!

Observations

Numerical simulation

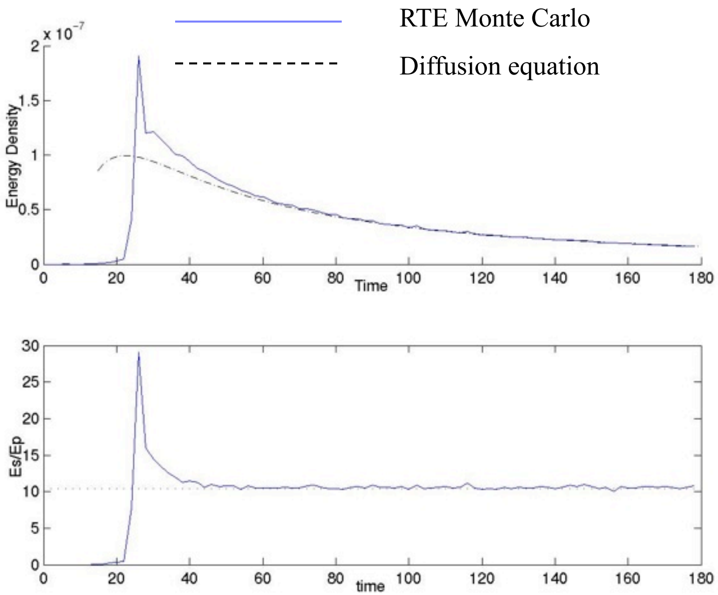

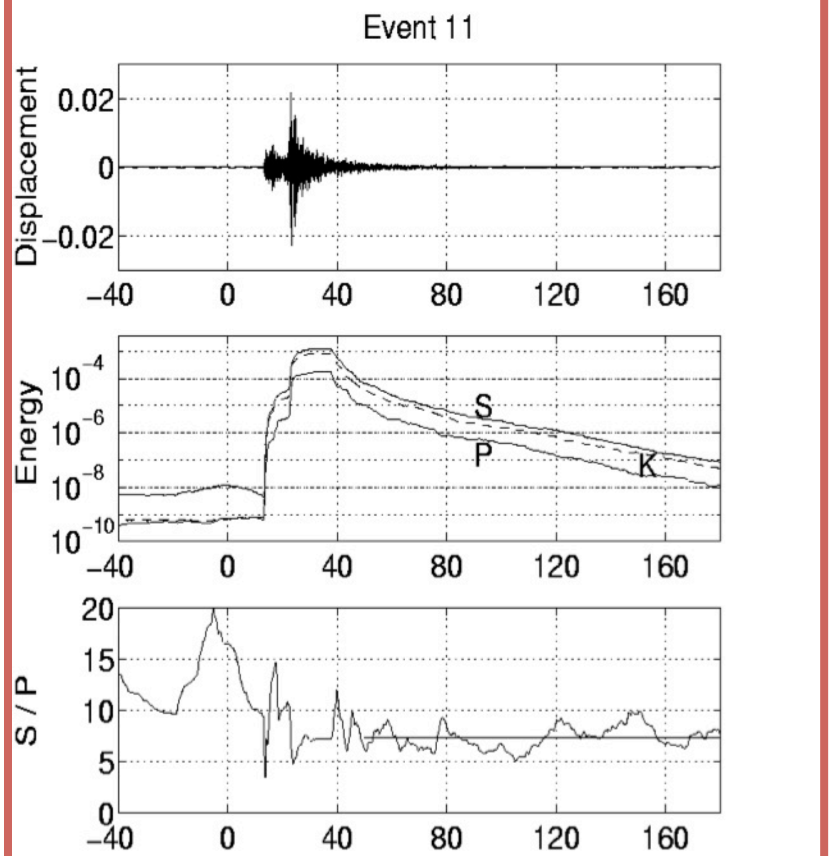

Infinite space
Energy ratio

$$2D: \quad E_S / E_P = \left(\frac{\alpha}{\beta}\right)^2 \qquad 3D: \quad E_S / E_P = 2.\left(\frac{\alpha}{\beta}\right)^3$$

Green function in 2D

P-SV case

$$G_{ij} = \frac{i}{4\rho\omega^2}\left\{-\delta_{ij}k^2 H_0^{(2)}(kr) + \frac{\partial^2}{\partial x_i \partial x_l}\left[H_0^{(2)}(qr) - H_0^{(2)}(kr)\right]\delta_{lj}\right\}$$

$$G_{ij}(P,Q) = \frac{-\mathrm{i}}{8\rho}\left\{A\delta_{ij} - B\left(2\gamma_i\gamma_j - \delta_{ij}\right)\right\} \qquad \gamma_j = \frac{x_j - \xi_j}{r}$$

$$A = \frac{H_0^{(2)}(qr)}{\alpha^2} + \frac{H_0^{(2)}(kr)}{\beta^2} \qquad B = \frac{H_2^{(2)}(qr)}{\alpha^2} - \frac{H_2^{(2)}(kr)}{\beta^2}$$

$$\alpha = \sqrt{\frac{\lambda + 2\mu}{\rho}} \qquad \beta = \sqrt{\frac{\mu}{\rho}} \qquad r = |P,Q|$$

THE 2D P-SVCASE $$\beta^2 \frac{\partial^2 u_i}{\partial x_j \partial x_j} + (\alpha^2 - \beta^2)\frac{\partial^2 u_j}{\partial x_i \partial x_j} = \frac{\partial^2 u_i}{\partial t^2}$$

Summation of P and S plane waves:

$$u_l(\mathbf{x}, \omega, t) = P(\omega, \phi) n_l \exp(-\mathrm{i}\frac{\omega}{\alpha} x_j n_j) + S(\omega, \psi) m_l^{;} \exp(-\mathrm{i}\frac{\omega}{\beta} x_j m_j)$$

Correlation:

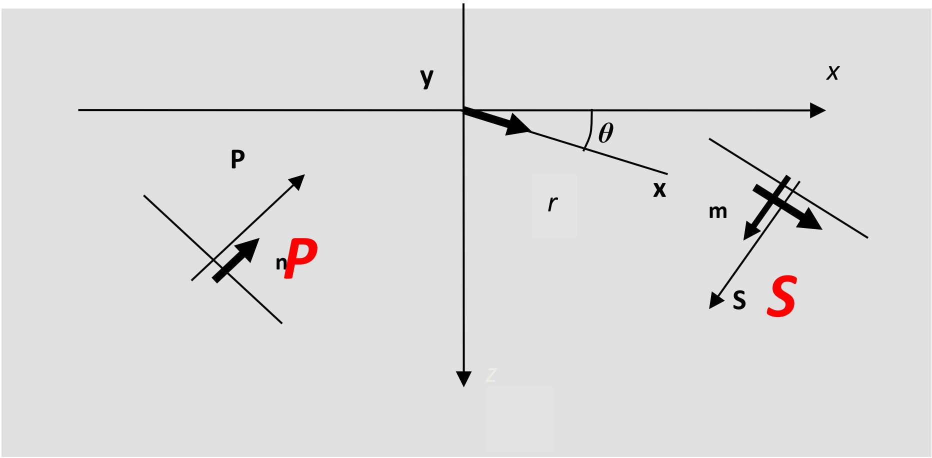

$$u_l(\mathbf{y}) u_s^*(\mathbf{x}) = (P^2 n_l n_s + SP^* m_l^{;} n_s)\exp(\mathbf{i}kr\cos[\varphi - \theta]) +$$
$$(S^2 m_l^{;} m_s^{;} + PS^* n_l m_s^{;})\exp(\mathbf{i}kr\cos[\psi - \theta])$$

Azimuthal average assuming: $P^2\alpha^2 = \varepsilon S^2\beta^2$

$$\langle \bullet \rangle = \frac{1}{4\pi^2}\int_0^{2\pi} d\phi \int_0^{2\pi} \bullet \, d\psi$$

$$\langle u_i(\mathbf{y})u_j^*(\mathbf{x})\rangle = \frac{S^2\beta^2}{2}\left\{A\delta_{ij} - B(2\gamma_i\gamma_j - \delta_{ij})\right\}$$

$$A = \varepsilon\frac{J_0(qr)}{\alpha^2} + \frac{J_0(kr)}{\beta^2} \text{ and } B = \varepsilon\frac{J_2(qr)}{\alpha^2} - \frac{J_2(kr)}{\beta^2}$$

And finally if ε=1, i.e. 2D equipartition ratio: $2D: \quad E_S / E_P = \left(\frac{\alpha}{\beta}\right)^2$

$$\boxed{\langle u_i(\mathbf{y},\omega)u_j^*(\mathbf{x},\omega)\rangle \equiv -8E_S k^{-2}\,\mathrm{Im}\left[G_{ij}(\mathbf{x},\mathbf{y},\omega)\right]}$$

Formally, same result in 3D (Sánchez-Sesma and Campillo, BSSA 2006)

Seismological application: coda waves

Individual cross-correlations:fluctuations dominate.

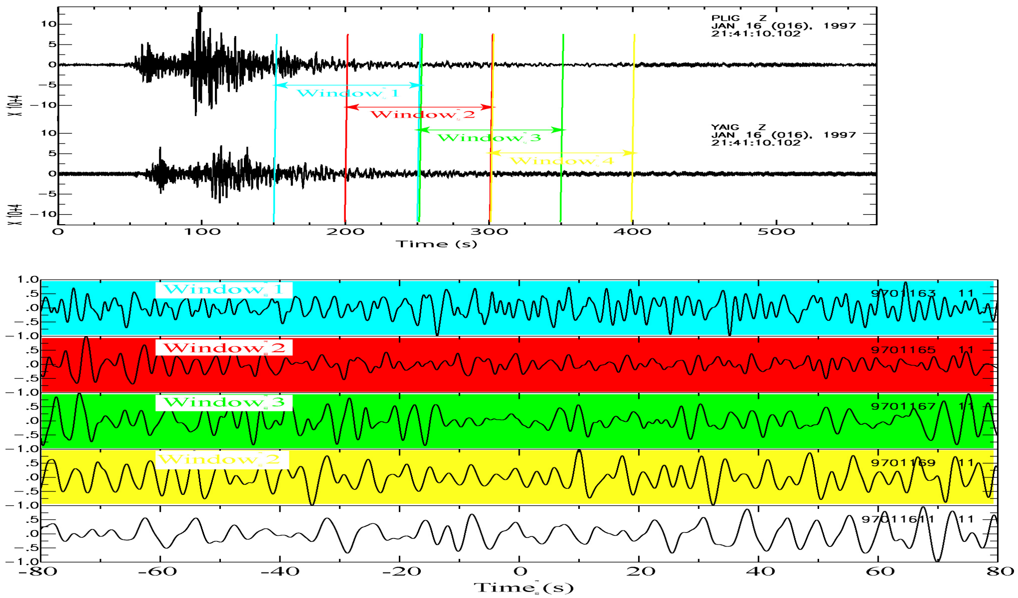

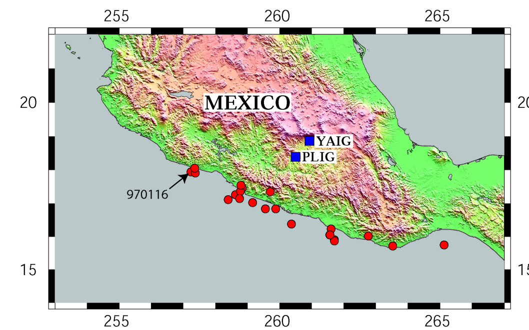

After averaging over 100 EQs➔

Emergence of the Green function

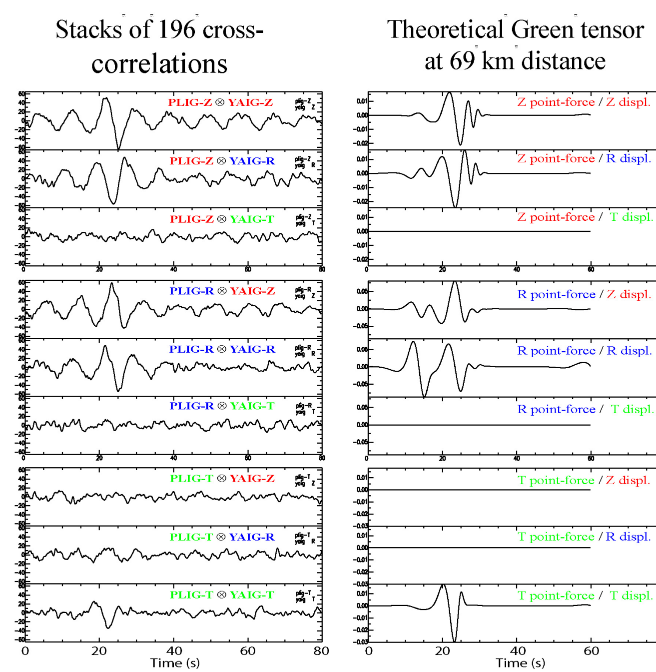

(Paul and Campillo, AGU 2001; Campillo and Paul, Science, 2003)

Cross-correlations of coda and noise records≈ Green functions = virtual seismograms

-demonstrated for the retrieval of surface waves (e.g. Paul and Campillo, 2001; Campillo and Paul, 2003; Shapiro and Campillo, 2004….) or body waves (e.g. Zhan et al., 2010 ; Poli et al., 2012).

High resolution velocity map of California obtained from ambient noise (Rayleigh)
(Shapiro, Campillo, Stehly and Ritzwoller, Science 2005)

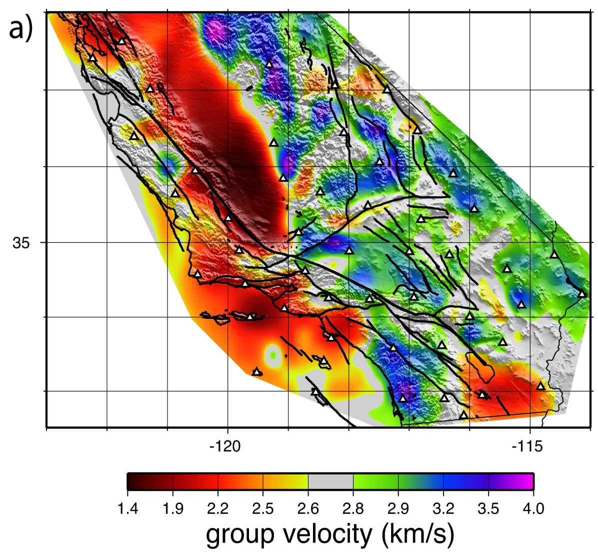

Earth's mantle discontinuities from ambient noise (phase transition ➔ (P,T))

Body waves (Poli et al., 2012)

Poli, Campillo, Pedersen. Science 2012

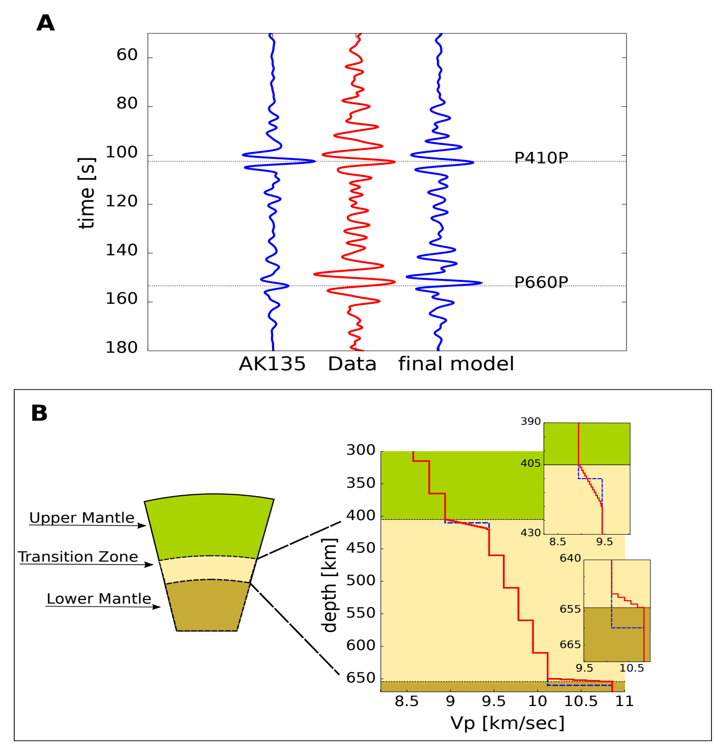

Large N sensor array =➔ $N^2/2$ correlations

Arbitrary medium: an integral representation written in the frequency domain

(see e.g. Weaver et al. 2004, or Snieder, 2007)

$$G_{12} - G_{12}^{*} = \boxed{\frac{4i\omega\kappa}{c}\int_{\mathcal{V}} G_{1x}G_{2x}^{*}\,dV} + \boxed{\oint_{S}\left[G_{1x}\vec{\nabla}\left(G_{2x}^{*}\right) - \vec{\nabla}\left(G_{1x}\right)G_{2x}^{*}\right]\overrightarrow{dS}}$$

Volume term

Surface term

FT of *G(-t)*

Absorption coefficient

FT of *G(t)*

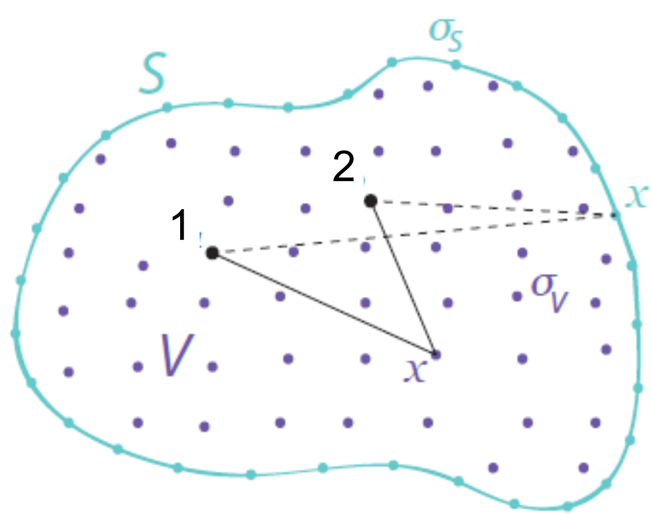

Helmholtz equation $G_{1x} = G(\vec{r}_1, \vec{x}; \omega)$

$$\Delta G_{1x} + V(\vec{x}) G_{1x} + (k + i\kappa)^2 G_{1x} = \delta(\vec{x} - \vec{r}_1)$$

where the potential $V(\vec{x})$ describes the scattering contribution does not extend to infinity.

As for the classical representation theorem, we consider a combination of the fields from source at 1 and 2 and compute the flux:

$$I = \oint_S \left[G_{1x} \vec{\nabla}\left(G_{2x}^*\right) - \vec{\nabla}\left(G_{2x}\right) G_{1x}^* \right] \overrightarrow{dS}$$

With the divergence theorem:

$$I = \int_{\mathcal{V}} \vec{\nabla}\left[G_{1x} \vec{\nabla}\left(G_{2x}^*\right) - \vec{\nabla}\left(G_{1x}\right) G_{2x}^* \right] dV$$

$$I = \int_{\mathcal{V}} \vec{\nabla}\left[G_{1x} \vec{\nabla}\left(G_{2x}^{*} \right) - \vec{\nabla}\left(G_{1x} \right) G_{2x}^{*} \right] dV$$

reduces to

$$I = \int_{\mathcal{V}} \left(G_{1x} \Delta G_{2x}^{*} - \Delta G_{1x} G_{2x}^{*} \right) dV$$

Using the definition of the GF:

$$\Delta G_{1x} = \delta\left(\vec{x} - \vec{r}_1 \right) - V\left(\vec{x} \right) G_{1x} - \left(k + i\kappa \right)^2 G_{1x}$$

we obtain:

$$I = G_{12} - G_{21}^{*} - \frac{4i\omega\kappa}{c} \int_{\mathcal{V}} G_{1x} G_{2x}^{*} \, dV$$

and finally:

$$G_{12} - G_{12}^{*} = \frac{4i\omega\kappa}{c} \int_{\mathcal{V}} G_{1x} G_{2x}^{*} \, dV + \oint_{S} \left[G_{1x} \vec{\nabla}\left(G_{2x}^{*} \right) - \vec{\nabla}\left(G_{1x} \right) G_{2x}^{*} \right] \overrightarrow{dS}$$

Representation theorem for correlation: passive imaging

Arbitrary medium: an integral representation written in the frequency domain

$$G_{12} - G_{12}^{*} = \frac{4i\omega\kappa}{c}\int_{V} G_{1x}G_{2x}^{*}\,dV + \oint_{S}\left[G_{1x}\vec{\nabla}\left(G_{2x}^{*}\right) - \vec{\nabla}\left(G_{1x}\right)G_{2x}^{*}\right]\overrightarrow{dS}$$

Volume term

Surface term

FT of $G(-t)$

FT of $G(t)$

Absorption coefficient

Source average over « correlation terms »

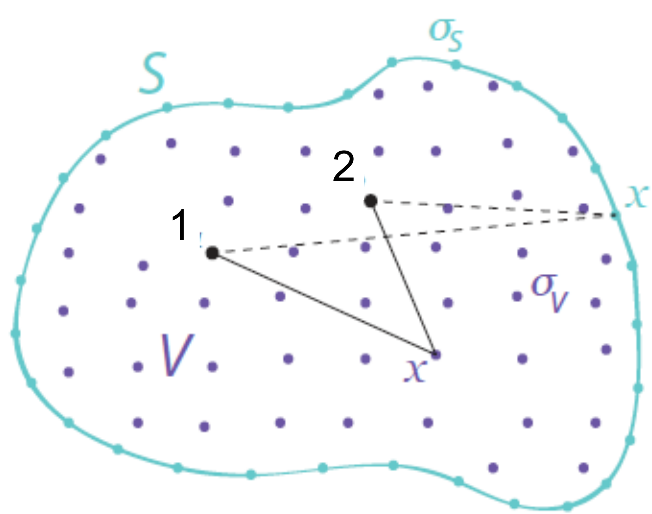

e.g. Weaver et al., 2004, Snieder 2007,….

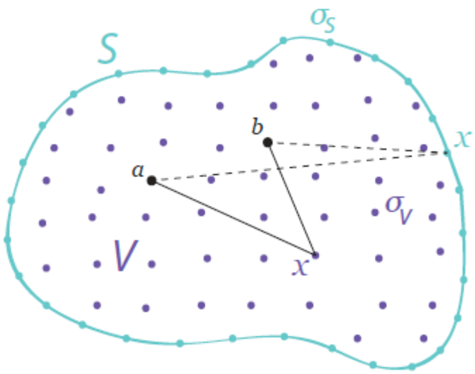

Volume term: $$G_{12} - G_{12}^{*} = \frac{4i\omega\kappa}{c} \int_{\mathcal{V}} G_{1x} G_{2x}^{*} \, dV$$

κ is finite (attenuation)

S is assumed to be sufficiently far away, for its contribution to be neglected (spreading and attenuation)

Surface term: $G_{12} - G_{12}^{*} = \oint_{S} \left[G_{1x} \vec{\nabla} \left(G_{2x}^{*} \right) - \vec{\nabla} \left(G_{1x} \right) G_{2x}^{*} \right] \overrightarrow{dS}$

κ =0 (no attenuation)

No source in the bulk

Surface term: $$\oint_S \left[G_{1x}\vec{\nabla}\left(G_{2x}^*\right) - \vec{\nabla}\left(G_{1x}\right)G_{2x}^* \right]\overrightarrow{dS}$$

If the surface is taken in the far field of the medium heterogeneities

$$G_{1x} \sim \frac{1}{4\pi\left|\vec{x}-\vec{r}_1\right|}\exp\left(-ik\left|\vec{x}-\vec{r}_1\right|\right) \text{ and } \vec{\nabla}\left(G_{1x}\right) \sim i\vec{k}\,G_{1x}$$

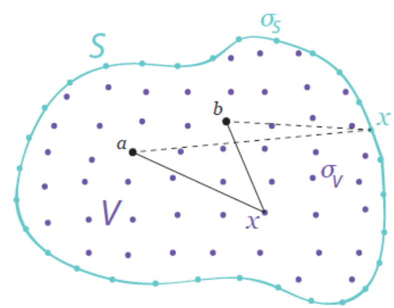

and we obtain a widely used integral relation:

$$\oint_S \left[G_{1x}\vec{\nabla}\left(G_{2x}^*\right) - \vec{\nabla}\left(G_{1x}\right)G_{2x}^* \right]\overrightarrow{dS} \approx -2i\frac{\omega}{c}\oint_S G_{1x}G_{2x}^*\,dS$$

Source average over
« correlation terms »

➔Derode et al., 2003: Analogy with Time reversal mirrors
➔Wapenaar 2004

For surface waves: distant sources of noise at the surface of the sphere (≈2D problem)

Location of the sources that contribute to the correlation: the end fire lobes

Difference of travel time between A and B
wrt the position of the source

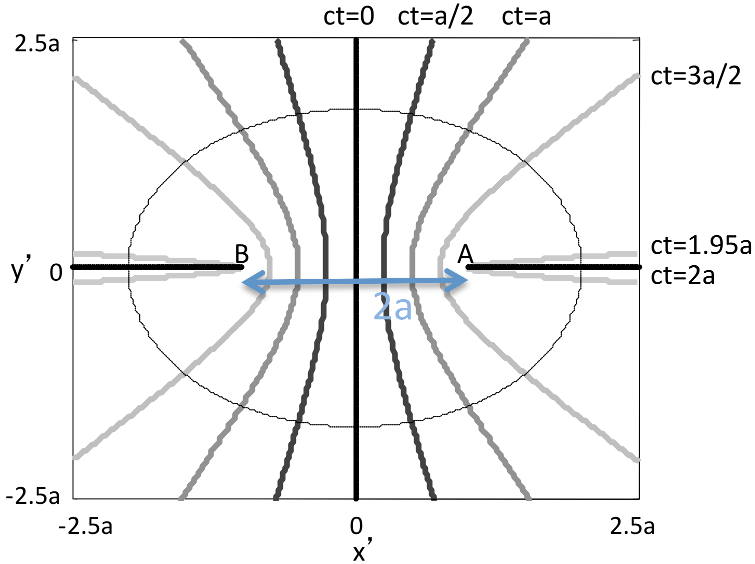

Stationary phase and end fire lobes

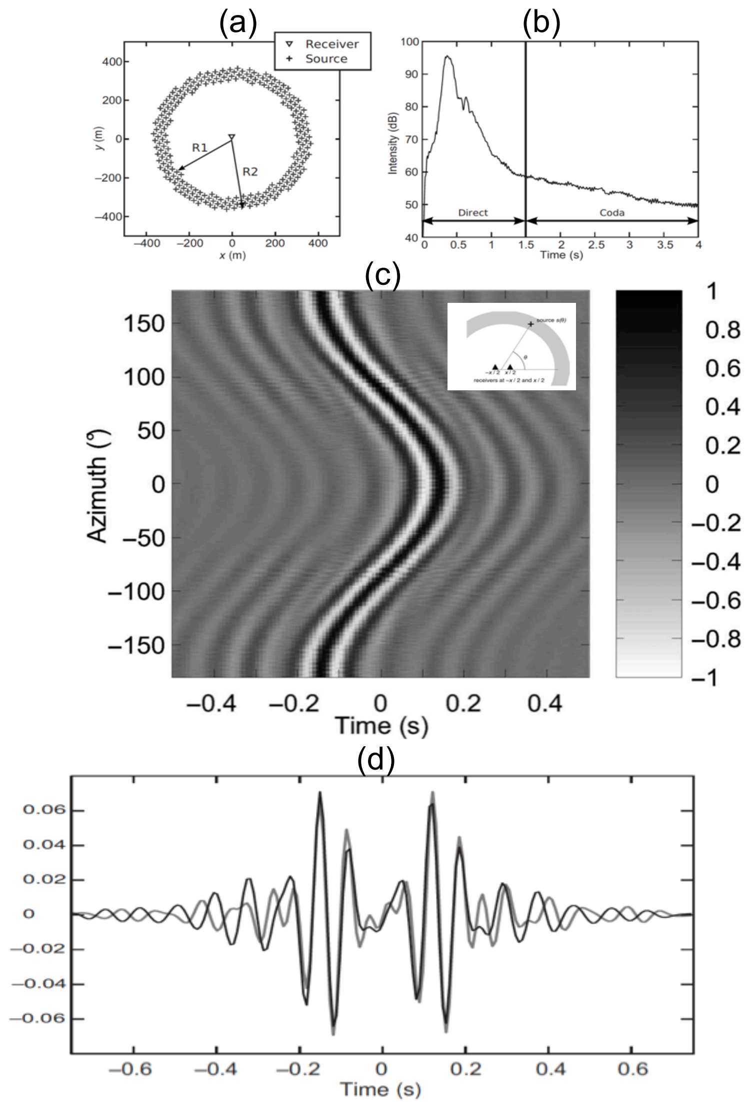

From Gouédard et al., 2009

End fire lobes

Contributions to direct waves in the GF

Scatterers or sources (Snieder, 2004; Roux et al., 2005)

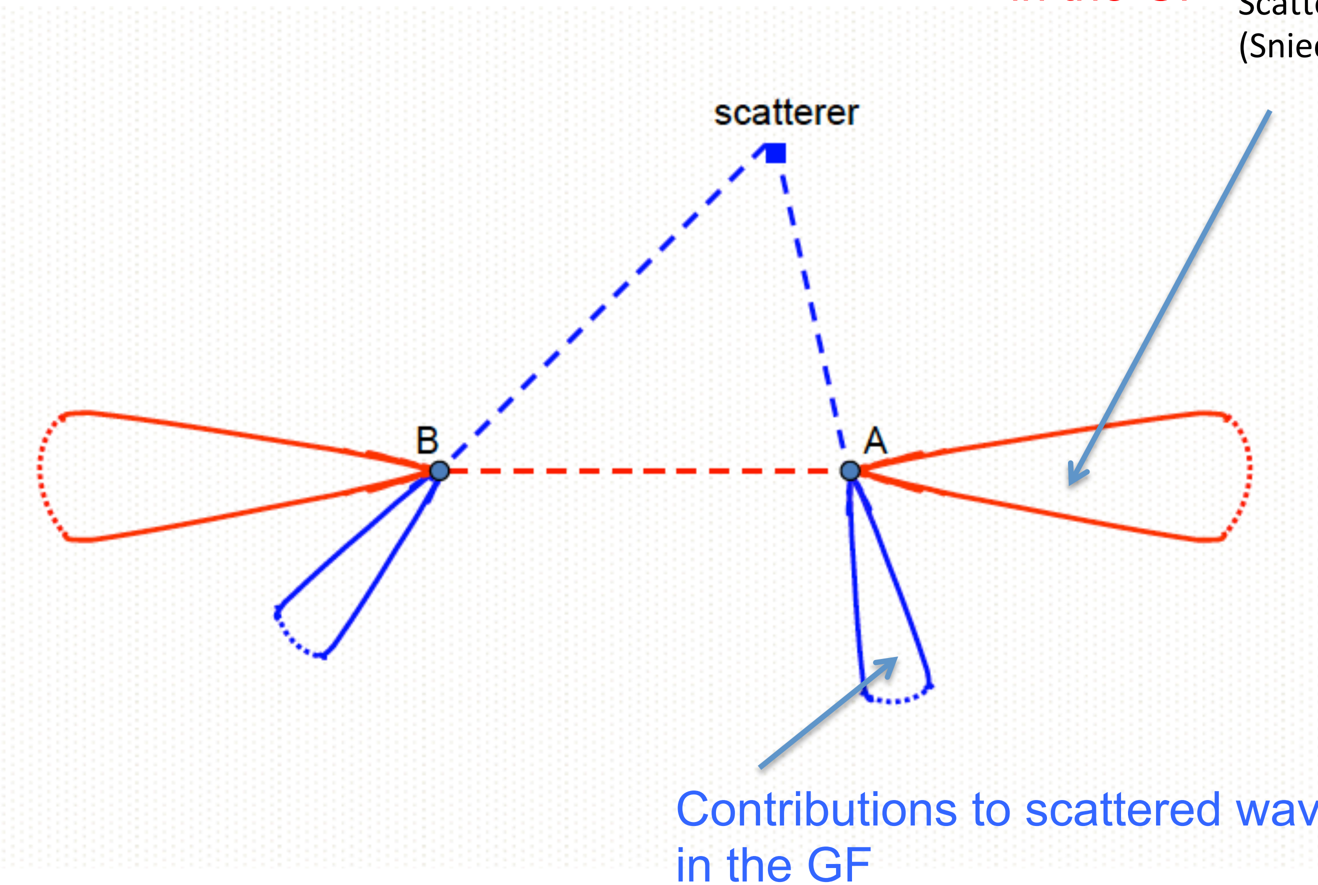

Contributions to scattered waves in the GF

Extension to scattered waves

Amplitude

Noise surface source kernels for causal at Rayleigh wave arrival time (From Stehly and Boué , 2016)

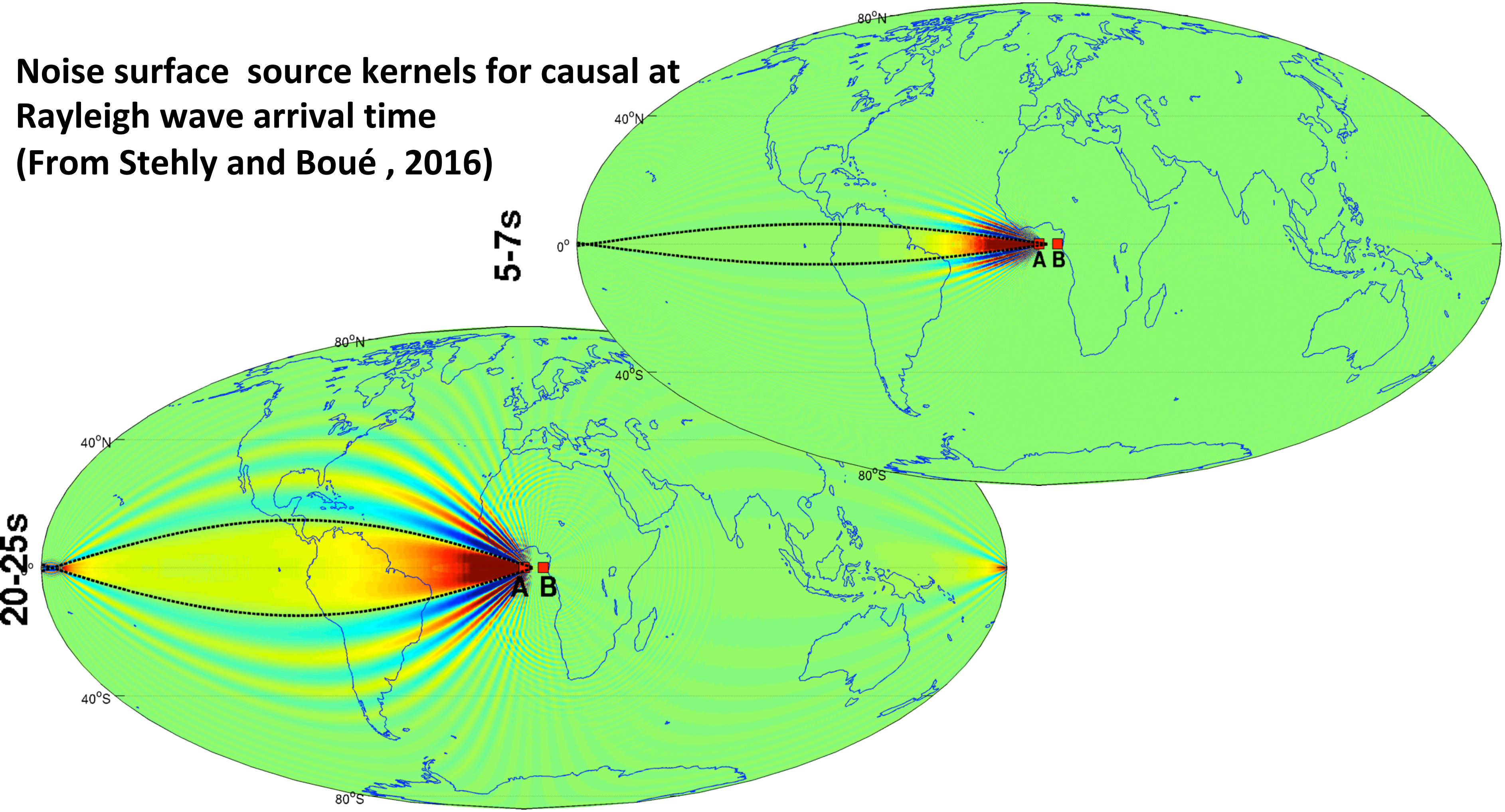

The kernels depends on frequency and interstation distance:

➔Difficulty for attenuation measurements

Problems and accuracy

Anisotropic intensity of the noise: the example of the San Jacinto fault

From Hillers et al., 2013 G3

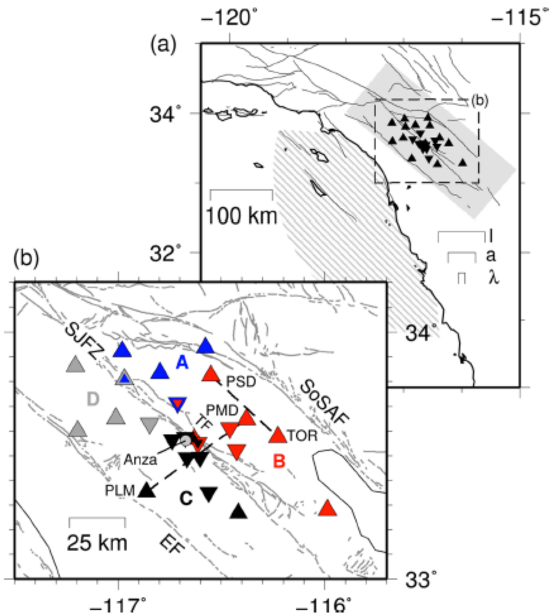

Anisotropic intensity of the noise

(measured for winter and summer and from different components)

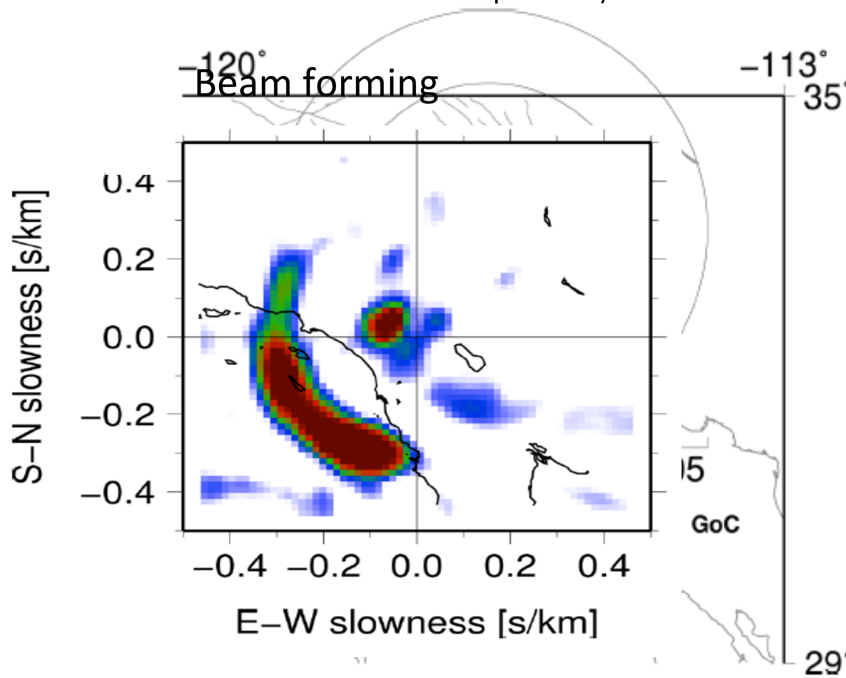

Correlation of direct waves:

Bias in the travel time

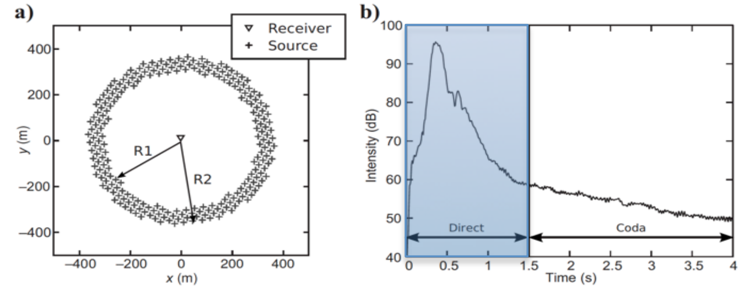

Increasing anisotropy of the source intensity *B*

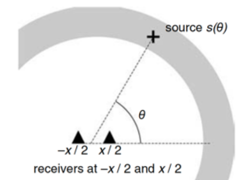

Azimuthal distribution of source intensity

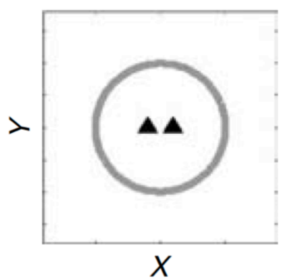

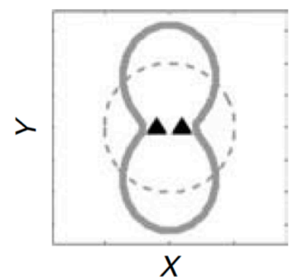

$$B(\theta) = 1 + B_2 \cos(2\theta)$$

Travel time error wrt the observed Green function

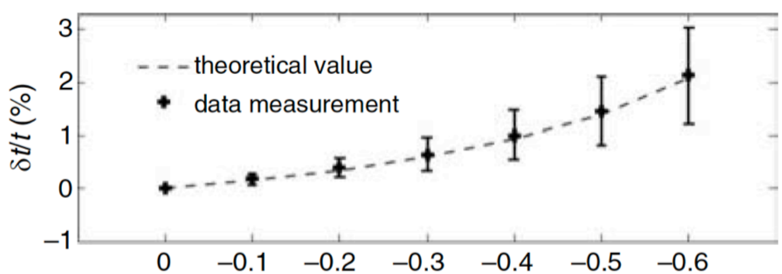

$$\delta t = \frac{1}{2t\,\omega_0^2 B(0)} \left.\frac{d^2 B(\theta)}{d\theta^2}\right|_{\theta=0}$$

valid with t (travel time) > T (period)

From Weaver, Froment, Campillo (2009) and Froment, Campillo, Roux, Gouédard, Verdel and Weaver 2011.

In presence of scattering:
Correlation of coda waves
-isotropy improvedby multiple scattering

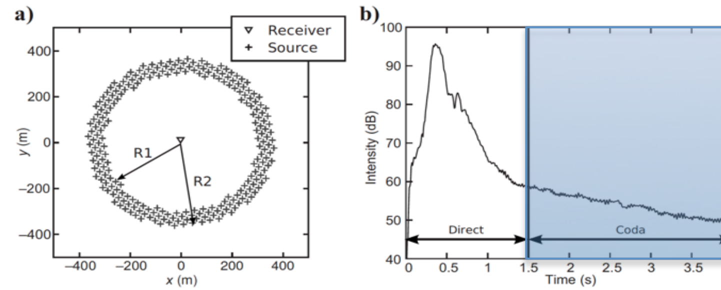

Increasing anisotropy of the source intensity *B*

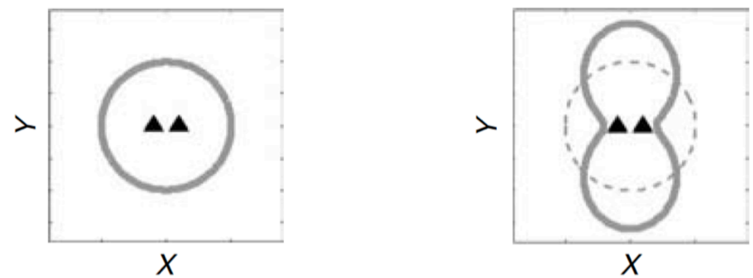

$$B(\theta) = 1 + B_2 \cos(2\theta)$$

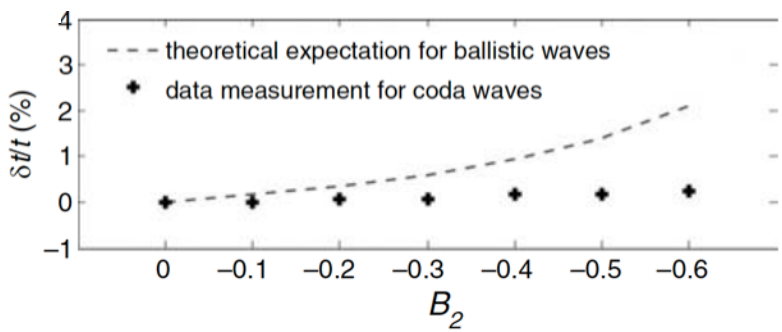

No bias in the correlation of coda waves!

From Froment, Campillo, Roux, Gouédard, Verdel and Weaver 2011.

In presence of scattering:
Correlation of coda waves
-isotropy provided by multiple scattering

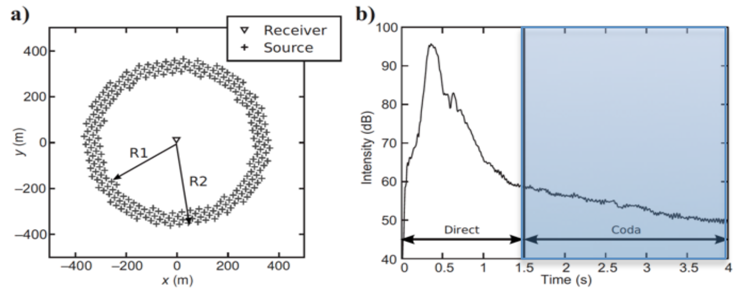

Increasing anisotropy of the source intensity *B*

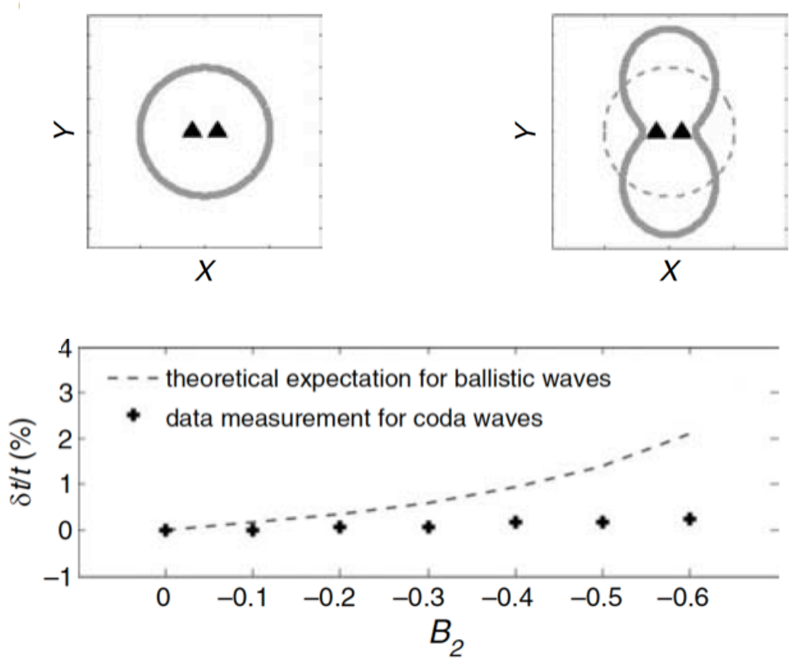

$$B(\theta) = 1 + B_2 \cos(2\theta)$$

Scattering provides the diversity of incidence directions ➔isotropization of intensity

No bias in the correlation of coda waves!

Noise records contain direct **<u>and</u>** scattered waves:

➔ the biases of direct wave travel times are generally small enough for imaging purpose

➔ Importance of processing strategies

From Froment, Campillo, Roux, Gouédard, Verdel and Weaver 2011.

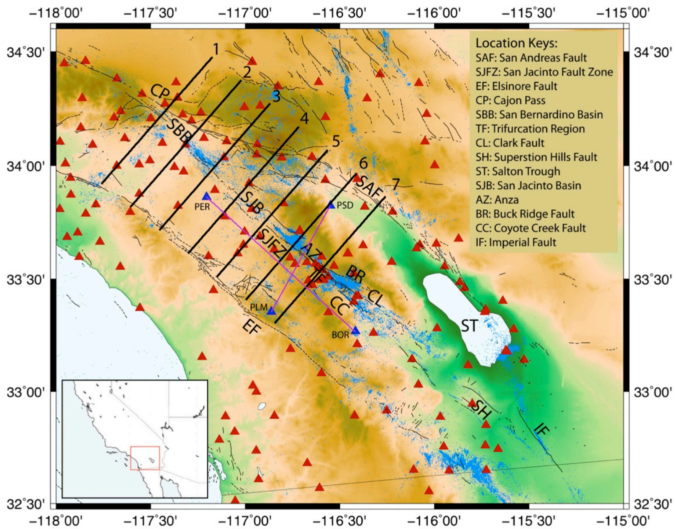

Shear wave tomography

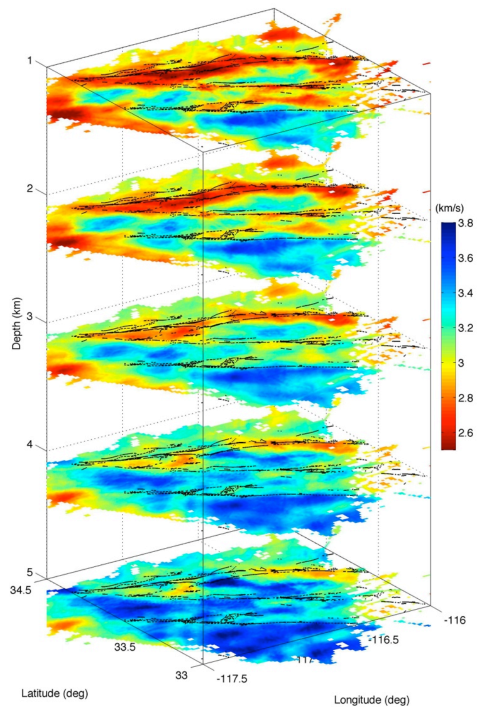

9-component correlations

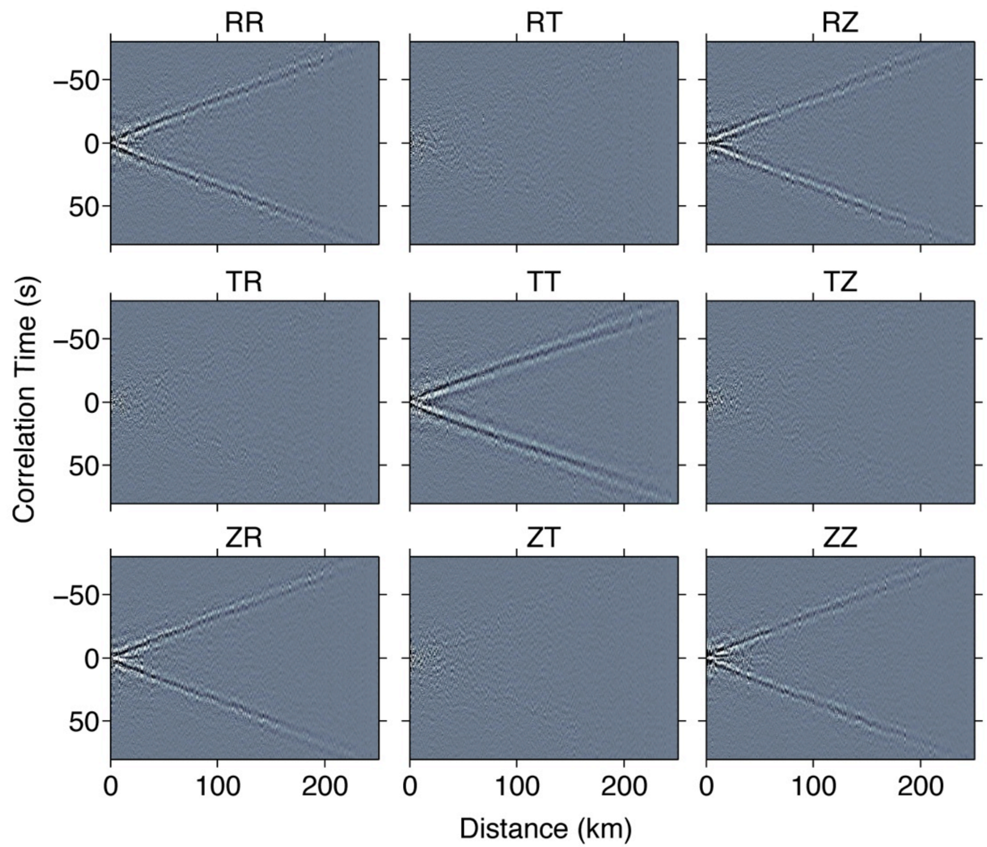

From Zigone, Ben-Zion, Campillo and Roux, 2014

Noise based seismic velocity temporal changes

Because seismic noise is continuous in time, it is possible to reconstruct **repeating virtual seismic sources** and perform **continuous monitoring of seismic velocities**.

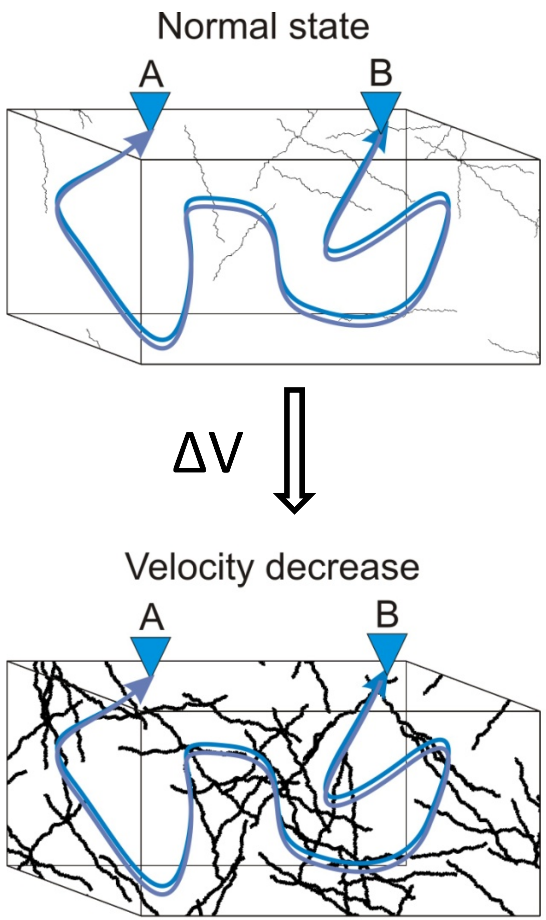

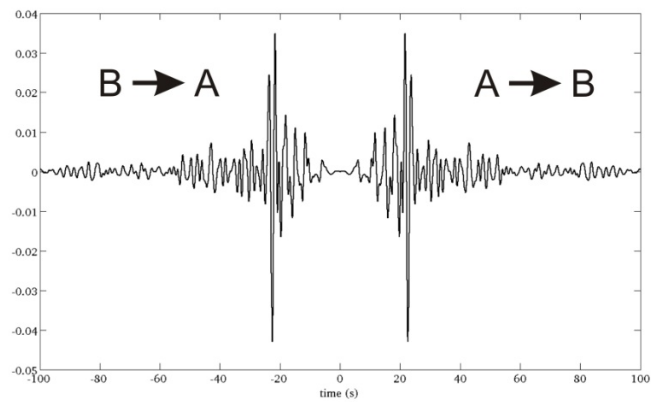

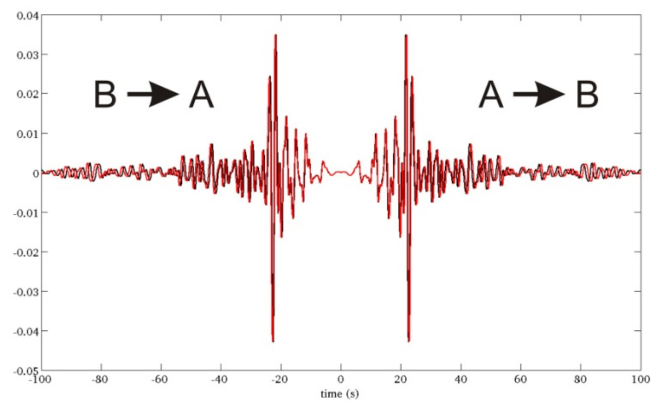

Correlation functions as approximate Green functions

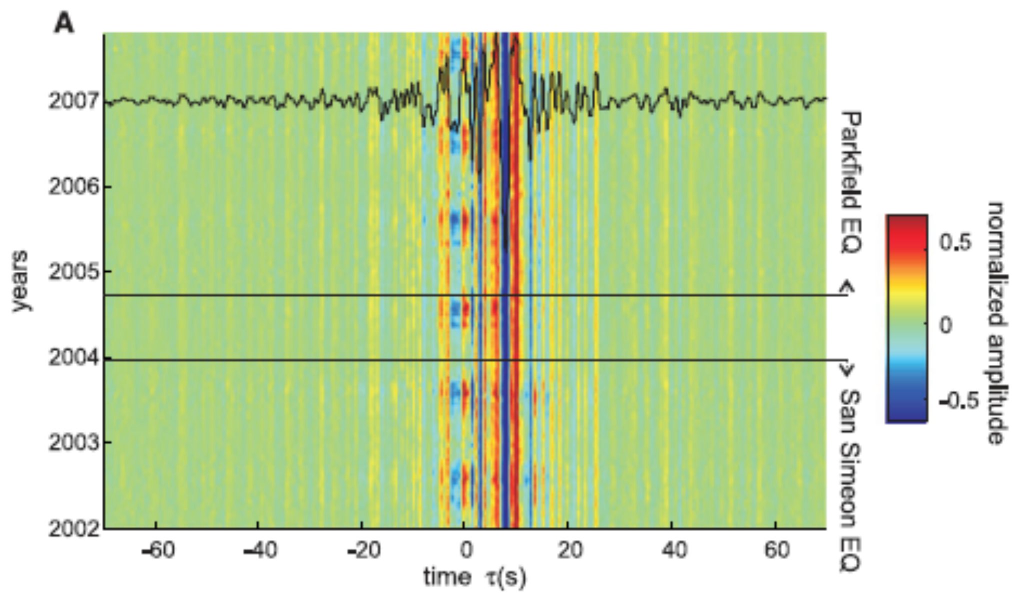

Direct waves are sensitive to noise source distribution (errors small enough for tomography (≤1%) but too large for monitoring (goal ≈ 10^{-4})

Stability of the ‘coda’ of the noise correlations

Detecting a small change of seismic speed: coda waves

Comparing a trace with a reference under the assumption of an homogeneous change

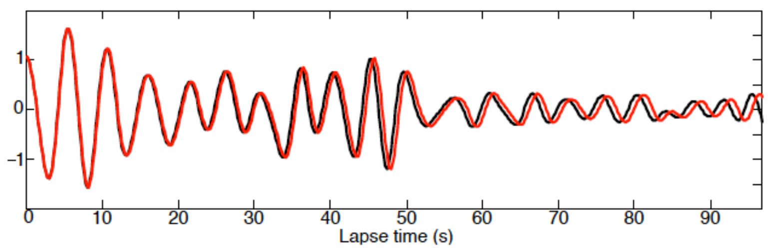

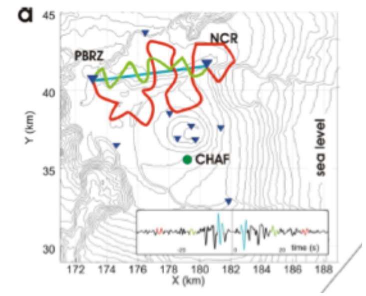

The ‘doublet’ method: moving window cross spectral analysis (phase measurements)

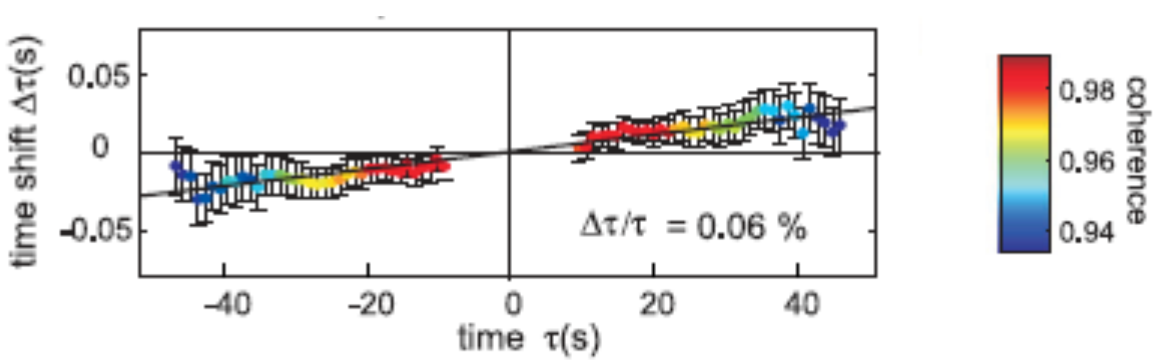

Alternative technique: stretching

Measuring slight changes of seismic velocity using coda waves (long travel time)
Numerical simulations in a scattering medium

2D spectral elements, anisotropic intensity of sources

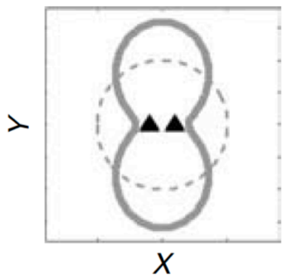

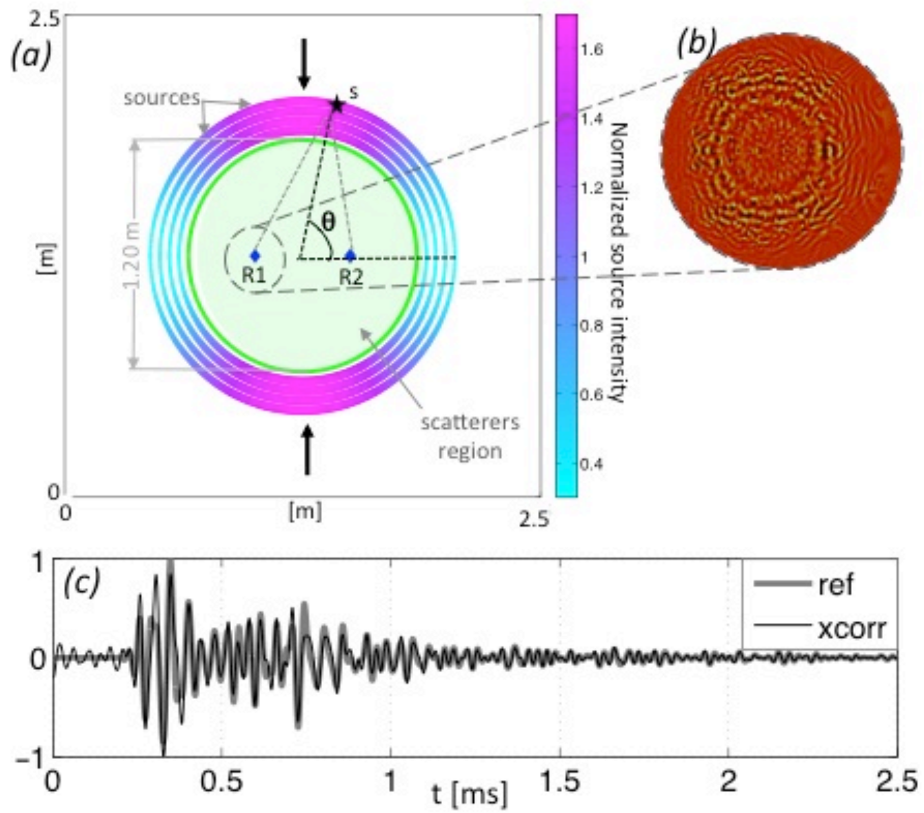

Comparison of correlations with Green function

Colombi, Chaput, Hillers et al., 2014 in press

Measure of the bias induced by a strong anisotropy
of the wave field
(delay with respect to the Green function)

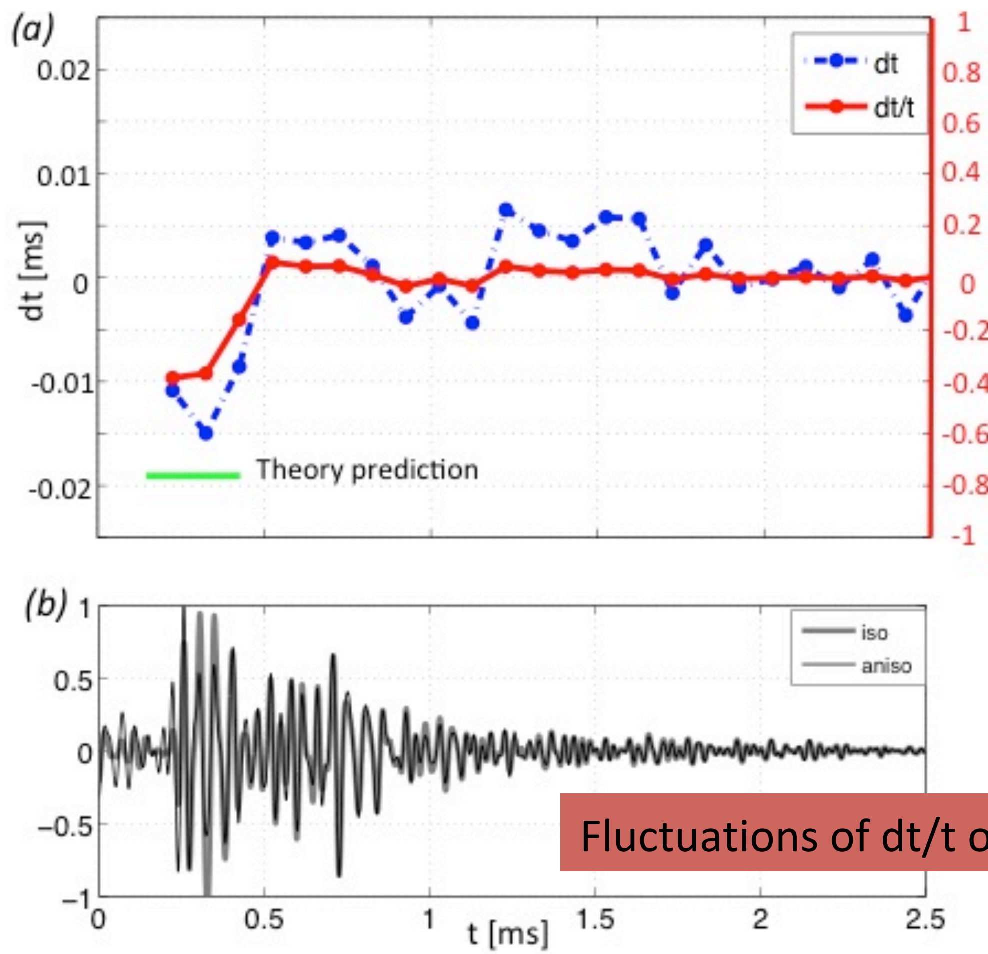

Blue: delay

Red: relative delay

Fluctuations of dt/t of the order of 10^{-4}

Colombi, Chaput, Hillers et al., 2014

Representation of coda waves as the sum of contributions of paths

For a single path:

$t_f = l_f / V$

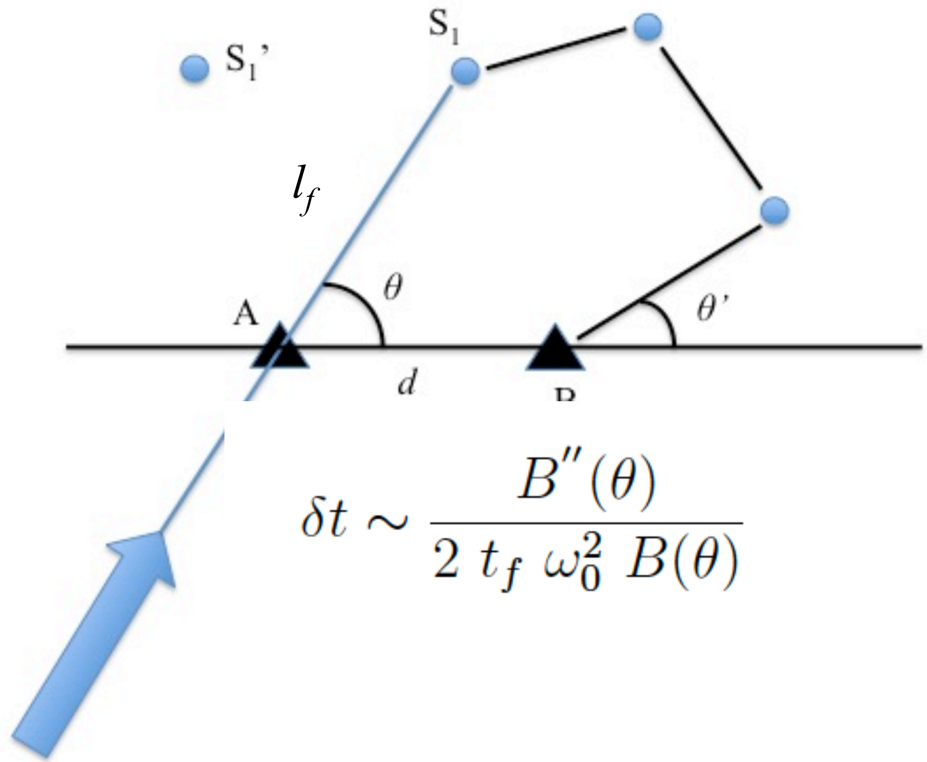

$$\delta t \sim \frac{B''(\theta)}{2\, t_f\, \omega_0^2\, B(\theta)}$$

We have to compute the contributions of paths with first scatterers at all distances l_f and all azimuths θ

We have to consider that the distribution of distance between scattering events is exponential:

$$P(l_f) = \frac{1}{l} e^{-\frac{l_f}{l}}$$ where l is the mean free path $$< l_f > = l \qquad t_f = l_f / V$$

We make use of $$\delta t \sim \frac{B''(\theta)}{2\ t_f\ \omega_0^2\ B(\theta)}$$ valid for $l_f > \lambda$

Applications

Numerical simulations

$$l = 0.5m,\ c = 2000\text{m/s},$$

$$f_0 = 30000\text{Hz},\ B_2 = -0.6 \text{ and } \tau_m = 0.002\text{s}$$

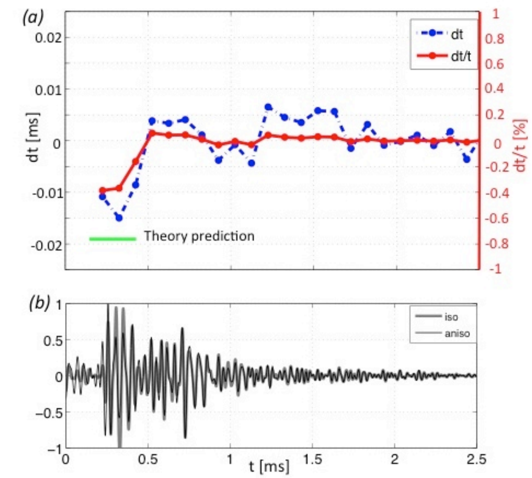

$\rightarrow$ fractional error $\frac{\delta t(\tau_m)}{\tau_m}$ of 10^{-4}

Seismic sensors in Japan….

Relative velocity change (in %) measured in the band 0.1-0.9 Hz

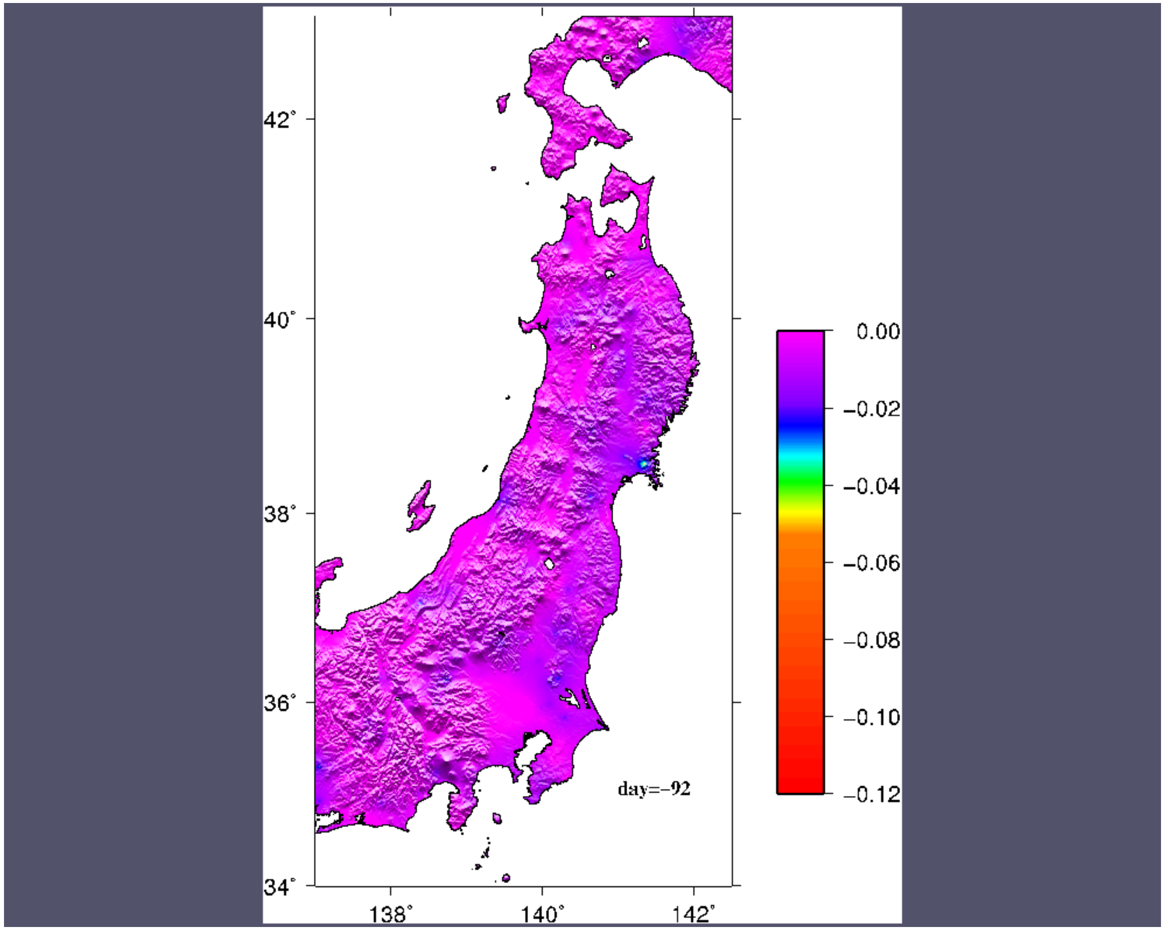

Calendar time measured in days with respect to March 11 (M9 Tohoku EQ)

Velocity change also observed for slow slip event (Rivet et al. 2011, 2014)

From Brenguier, Campillo, Takeda, Aoki, Shapiro, Briand, Emoto and Miyake, Science 2014

Seasonal changes of velocities and correction from external forcings

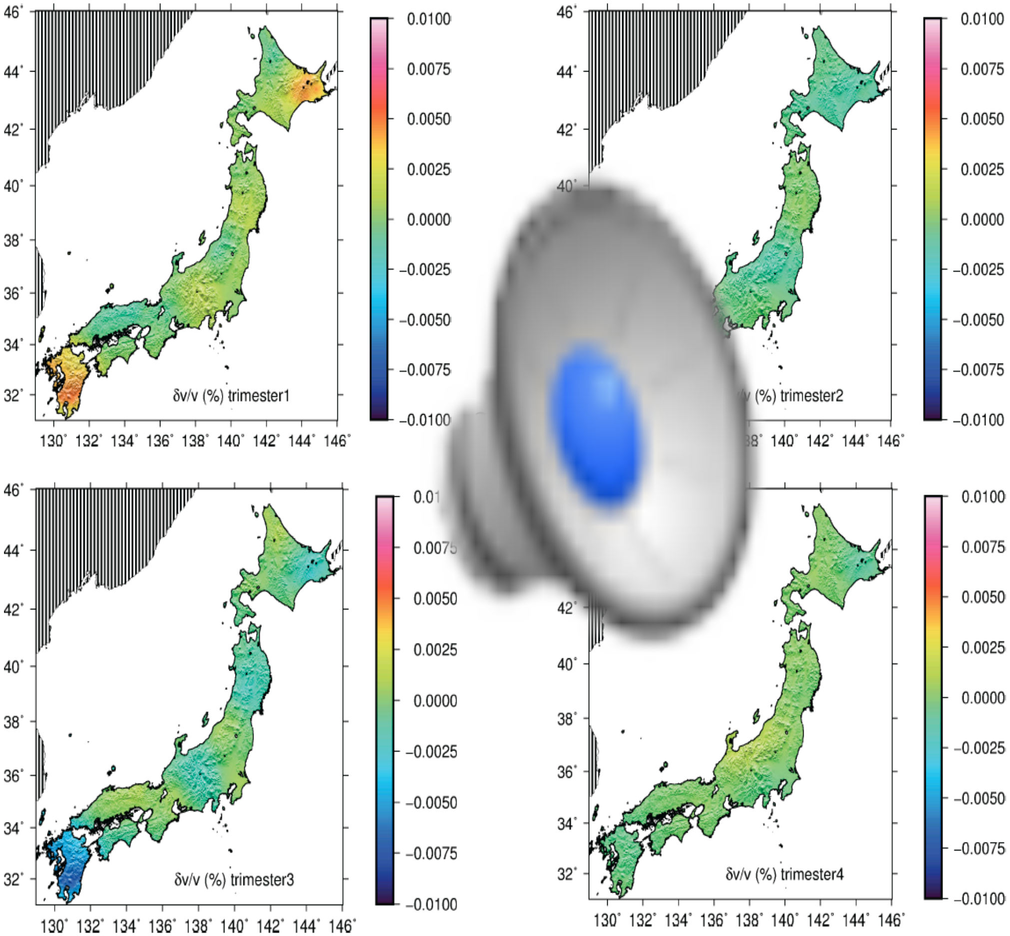

b)

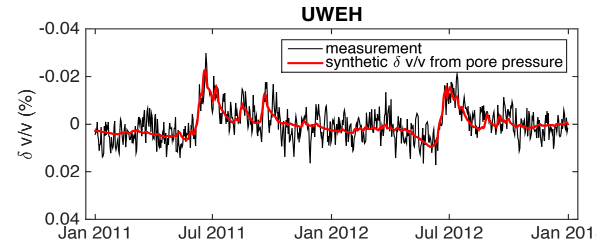

c)

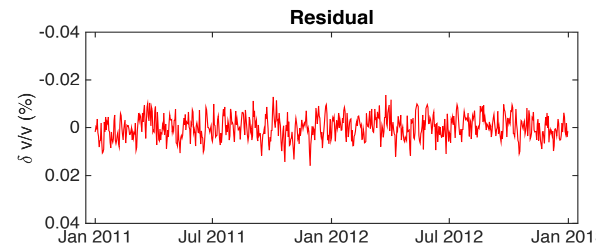

Smaller scale, industrial environment

Active mine: various sources of noise
tunnels (scattering)

Section view

Plan view

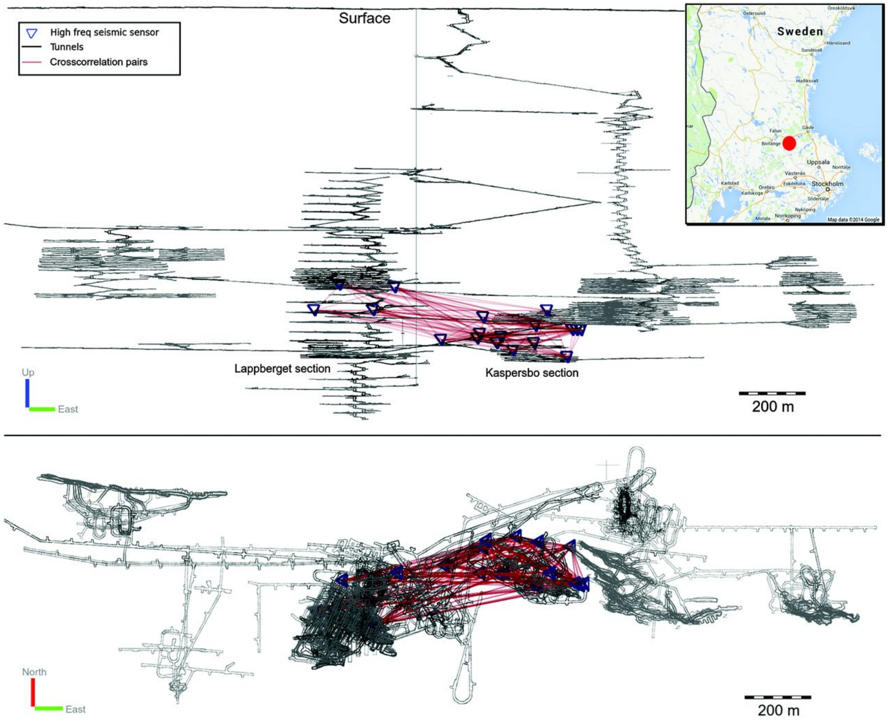

Results from Olivier, Brenguier, Campillo, Lynch and Roux, 2015
GEOPHYSICS, VOL. 80, NO. 3 (MAY-JUNE 2015); P. KS11–KS25

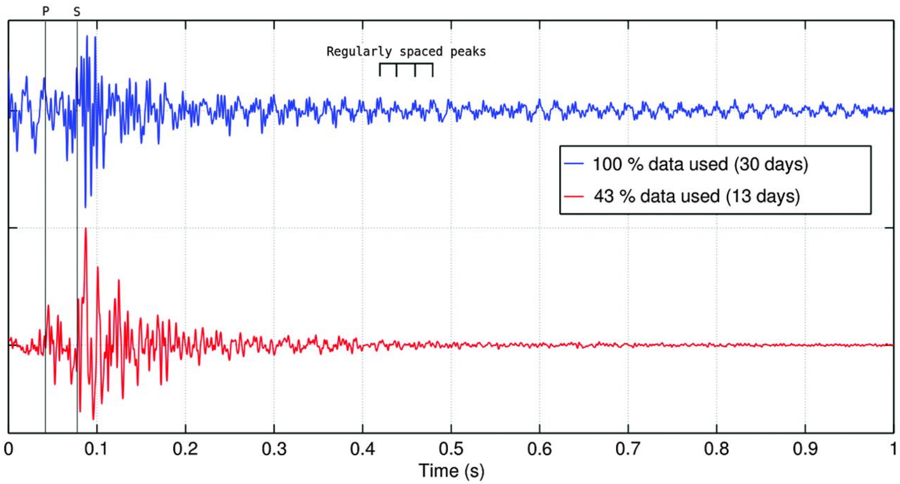

Correlation functions (ZZ)

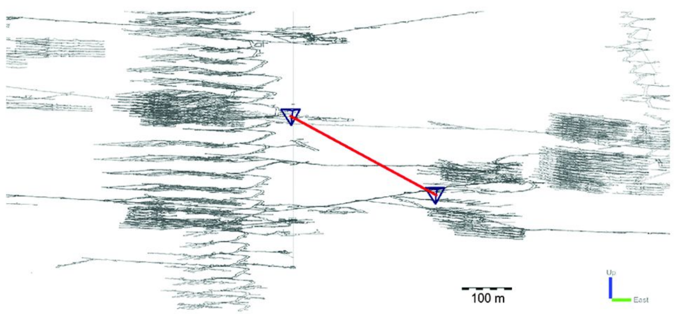

Scattering properties from noise correlations

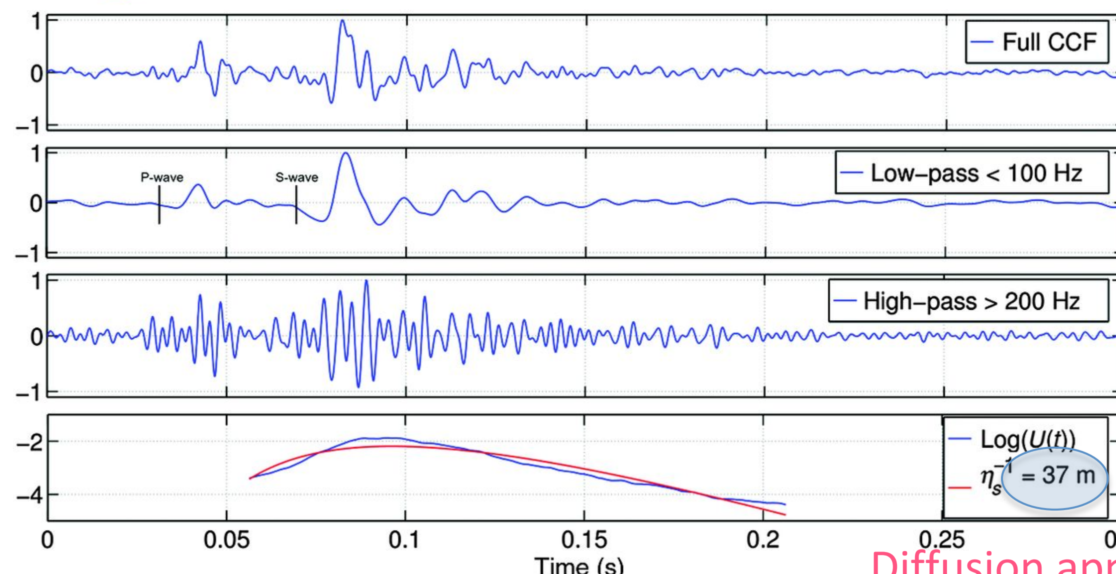

Diffusion approx.

Local scale

Velocity change due to blast and excavation in a mine

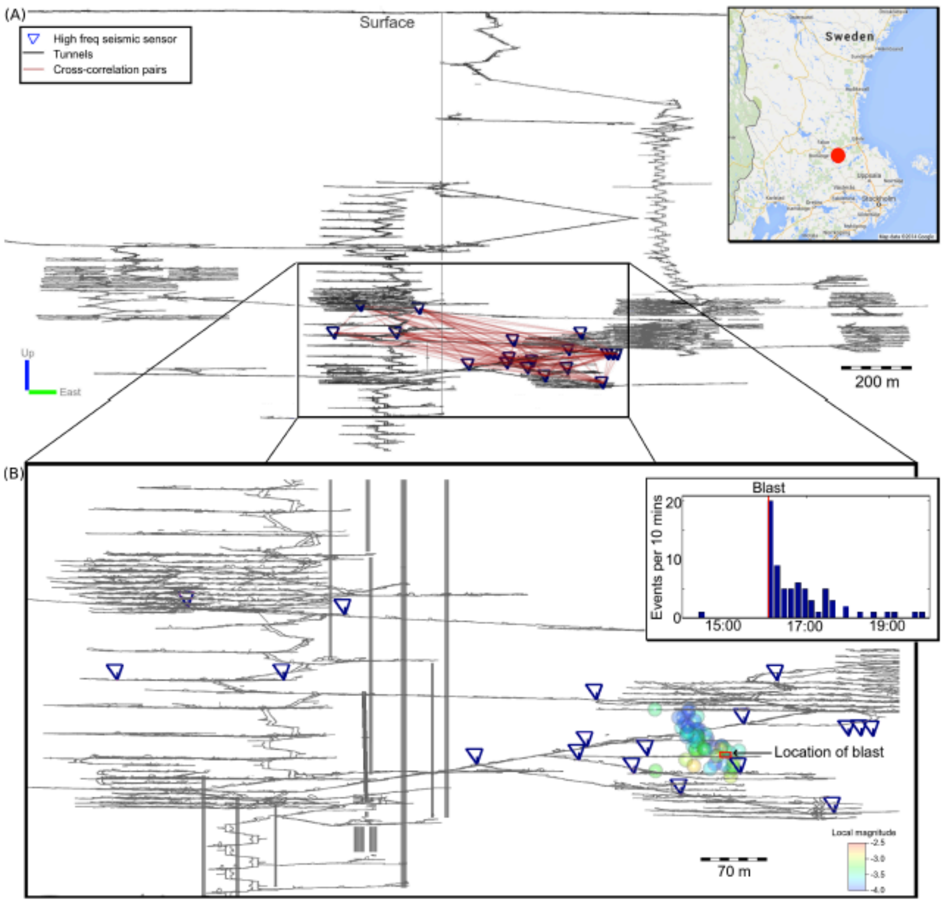

Use of the strong industrial noise in the mine.
Note the intense scattering associated with the tunnels.

Olivier et al., 2014

Velocity change due to blast and excavation in a mine

Fast dynamics

Slow dynamics

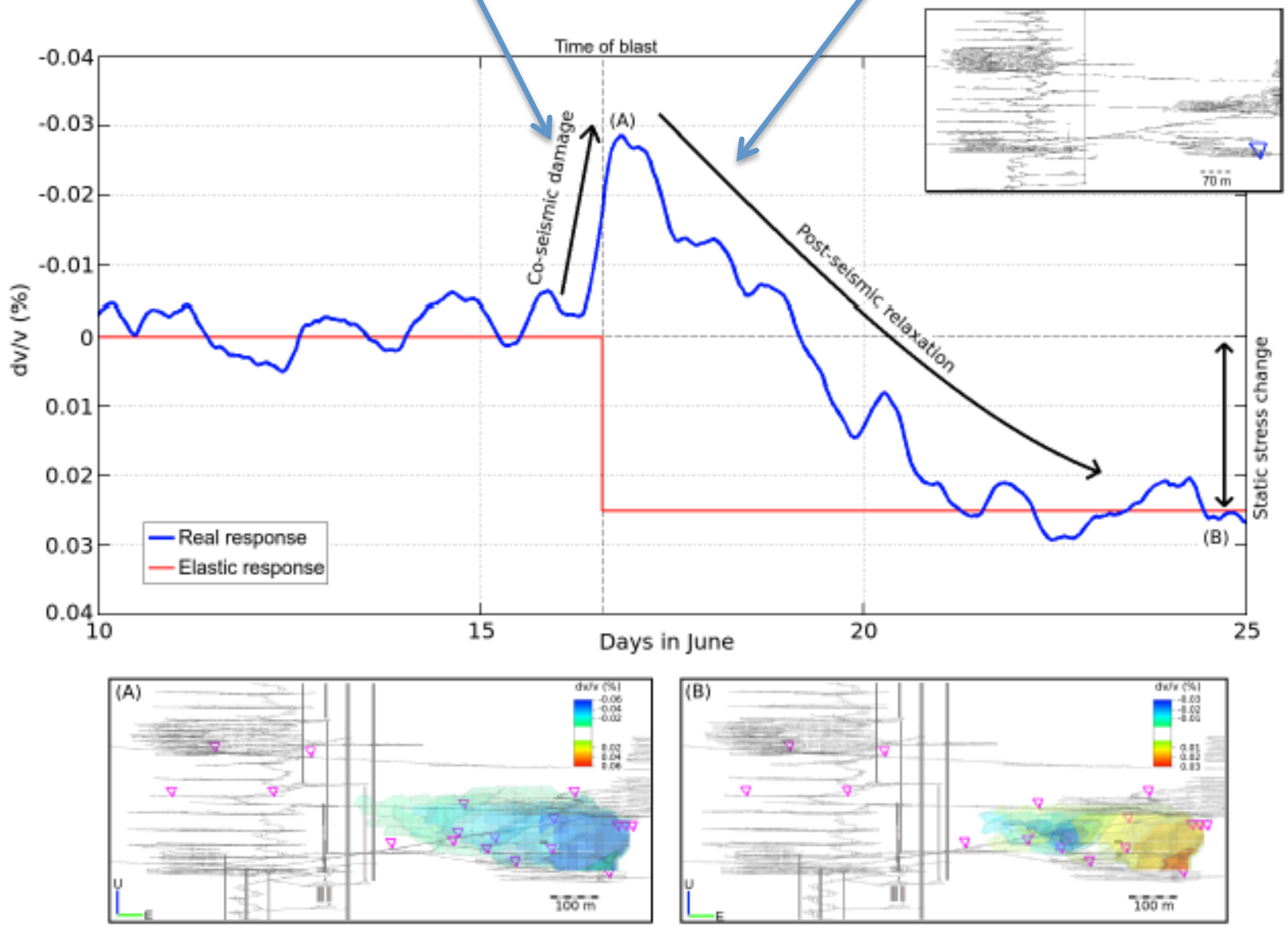

Change of baseline due to static stress change

Instantaneous change

Static change

From Gerrit Olivier and co-authors (2015)